PB-236 390

STUDY OF FACTORS AFFECTING REACTIONS IN ENVIRONMENTAL CHAMBERS

Raphael J. Jaffe, et al

Lockheed Missiles and Space Company, Incorporated

Prepared for:

Environmental Protection Agency
Coordinating Research Council, Incorporated

29 April 1974

DISTRIBUTED BY:

NTIS

National Technical Information Service
U. S. DEPARTMENT OF COMMERCE

BIBLIOGRAPHIC DATA SHEET	1. Report No. CRC-APRAC-CAPA-1-69-2	2.	PB 236 390

4. Title and Subtitle

Study of Factors Affecting Reactions in Environmental Chambers -- Phase II

5. Report Date: April 29, 1974

6.

7. Author(s): R. J. Jaffe, F. C. Smith, Jr., and K. W. Last

8. Performing Organization Rept. No. LMSC-D401598

9. Performing Organization Name and Address: Lockheed Missiles & Space Company, Inc., Sunnyvale, California 94088

10. Project/Task/Work Unit No. CRC-APRAC-CAPA-1-69

11. Contract/Grant No.

12. Sponsoring Organization Name and Address: Coordinating Research Council, Inc, 30 Rockefeller Plaza, New York, New York 10020 and Environmental Protection Agency, Research Triangle Park, North Carolina 27711

13. Type of Report & Period Covered: Final -- Phase II

14.

15. Supplementary Notes: Not releasable to the general public until October 1, 1974.

16. Abstracts

The effects of materials, spectra, surface to volume ratio (S/V) and cleaning techniques on the photochemical reactions observed in an environmental chamber were studied using a unique chamber and lighting system. The study included four materials (aluminum, Pyrex, Teflon, and stainless steel) and two conditions each of spectrum, S/V, and cleaning. All photochemical runs are at K_d of 0.3 min^{-1} as determined by frequent NO_2 in N_2 photolysis tests. The time to NO_2 maximum was found to occur fastest in a chamber of stainless steel followed in order by aluminum, Pyrex and Teflon. Maximum ozone concentration increase in the order: stainless steel, Pyrex, aluminum, Teflon. Using a spectrum cutting out energy below 340 nm wavelength, strikingly lowers reaction rates compared to the full spectrum. S/V was also found to measurably affect the reactions. Using the two cleaning techniques there was little difference in drawing off the chamber gases in a high-vacuum space chamber or in purging the chamber with pure air.

17. Key Words and Document Analysis. 17a. Descriptors

Irradiation Chamber
Illuminator
NO_2-NO_x
Ozone
Total Hydrocarbons
Propylene
Acetaldehyde
Peroxyacetyl Nitrate (PAN)
Photochemical
Aluminum
Stainless Steel
Spectra
Smog

17b. Identifiers/Open-Ended Terms

Pyrex
Teflon

Reproduced by
NATIONAL TECHNICAL
INFORMATION SERVICE
U S Department of Commerce
Springfield VA 22151

17c. COSATI Field/Group: 07C; 07E; 07B; 20F; 04B; 13B.

18. Availability Statement: Releasable to the general public.

19. Security Class (This Report) UNCLASSIFIED

20. Security Class (This Page) UNCLASSIFIED

21. No. of Pages: 83

22. Price: 4.00 - 6.50

FORM NTIS-35 (REV. 3-72)
THIS FORM MAY BE REPRODUCED
USCOMM-DC 14952-P72

LMSC-D401598
April 29, 1974

Study of

FACTORS AFFECTING REACTIONS IN ENVIRONMENTAL CHAMBERS

Final Report – Phase II

by Raphael J. Jaffe, Frank C. Smith, Jr., and K. W. Last

Prepared for
COORDINATING RESEARCH COUNCIL
New York, N.Y.
Under Contracts CAPA 1-69(1-72) and (1-73)

and

ENVIRONMENTAL PROTECTION AGENCY
Research Triangle Park, North Carolina
Under Contract 68-02-0287

Biotechnology
Lockheed Missiles & Space Company, Inc.
Sunnyvale, California

SUMMARY

An experimental study has been conducted of effects of materials, spectrum, surface/volume ratio (S/V) and cleaning technique on the photochemical reactions observed in a smog chamber. A unique chamber and lighting system was used, which permitted independent variation in chamber materials and in light conditions. A xenon arc lamp parabolic reflector combination provided a collimated light beam. By orienting plates of materials parallel to the beam, it has been possible to independently vary light conditions and materials.

The study included four materials – aluminum, Pyrex, Teflon, and stainless steel, and two conditions each of spectrum, S/V, and cleaning. A complete factorial testing sequence was performed. All photochemical runs were at k_d of 0.3 min^{-1} as determined by frequent NO_2 in N_2 photolysis tests. The propylene (3 ppm)/NO_x (1.5 ppm) reaction system was used, at 95° F and 25% relative humidity. Initial NO_2 content was nominally 10% of NO_x. Chamber background was < 0.1 ppm C.

Effects of the different materials and of the two levels of each parameter have been determined. The time to NO_2 maximum is shortest for stainless steel followed by aluminum, Pyrex and Teflon, in order. Maximum ozone concentration increases in the order: stainless steel, Pyrex, aluminum, Teflon. Stainless steel behaves in a manner unlike the other three materials.

The cutoff spectrum (little energy below 340 nm wavelength) strikingly lowers reaction rates compared to the full spectrum. Surface/volume ratio measurably affects the reactions. The variations in the two cleaning techniques do not affect as many of the run characteristics. The presence of this large spectral effect (at constant k_d) was not anticipated, and cannot be explained in a simple manner.

PROJECT PERSONNEL

Name	Area of Contribution
Raphael J. Jaffe	Project Direction
Frank C. Smith, Jr.	Analytical Chemistry/Chamber Operation
Ken W. Last	Statistical Analysis
E. H. Kawasaki	Analytical Chemistry
R. C. Tuttle	Analytical Chemistry
Dr. H. S. Johnston, Consultant	Photochemistry

PROJECT MONITORSHIP
COORDINATING RESEARCH COUNCIL
PROJECT CAPA 1-69

Member	Affiliation
Mr. D. B. Wimmer, Chairman	Phillips Petroleum Company
Mr. Frank Bonamassa	California Air Resources Board
Mr. Basil Dimitriades	Environmental Protection Agency
Dr. J. M. Heuss	General Motors Corporation
Mr. Stanley Kopezynski*	Environmental Protection Agency
Dr. Hiromi Niki	Ford Motor Company
Dr. E. E. Wigg	Esso Research & Engineering Company

*Until January 1973

CONTENTS

Section		Page
	ILLUSTRATIONS	vii
1	INTRODUCTION	1-1
2	EXPERIMENTAL METHOD	2-1
	2.1 Test Conditions	2-1
	2.2 Apparatus	2-2
	2.2.1 Irradiation Chamber	2-2
	2.2.2 Illuminator	2-8
	2.2.3 Thermal Enclosure	2-9
	2.2.4 Material and S/V Changes	2-11
	2.2.5 Spectral Distribution and Spectral Changes	2-13
	2.2.6 Cleaning Technique	2-15
	2.2.7 Chamber Charging Technique	2-17
	2.3 Chemical Analysis Methodology	2-17
	2.3.1 NO_2-NO_x	2-17
	2.3.2 Ozone	2-19
	2.3.3 Total Hydrocarbons	2-21
	2.3.4 Propylene	2-22
	2.3.5 Acetaldehyde	2-22
	2.3.6 Peroxyacetyl Nitrate (PAN)	2-22
	2.3.7 Moisture (Water)	2-23
3	RESULTS	3-1
	3.1 Material Differences	3-10
	3.2 Effect of Factors	3-10
	3.3 Ozone Decay Results	3-11
4	DISCUSSION	4-1

Section		Page
5	FUTURE WORK	5-1
	5.1 Ongoing Work	5-1
	5.2 Recommended Further Work	5-1
	REFERENCES	R-1

ILLUSTRATIONS

Figure		Page
2-1	Smog Chamber Assembly	2-4
2-2	Stand Assembly	2-6
2-3	Environmental Chamber Showing Side Stream Mixer, Charge Ports, and Clean-Out Port	2-7
2-4	Chamber Inside Thermal Enclosure	2-10
2-5	Arrangement of Surface Plates	2-12
2-6	Measured Spectral Irradiance Inside LMSC Smog Chamber-Full and Cut Spectra	2-14
2-7	Typical Raw Data for Determining k_d	2-15
2-8	Smog Chamber During Vacuum Off-gassing Cleaning	2-16
2-9	Typical Linearity Check of NO Instrument	2-20
3-1	Composite Photochemical Test Results for Teflon Film Surfaces	3-5
3-2	Composite Photochemical Test Results for Pyrex Surfaces	3-5
3-3	Composite Photochemical Test Results for Aluminum Surfaces	3-5
3-4	Composite Photochemical Test Results for Stainless Steel Surfaces	3-5
4-1	Distribution of NO_2 Photodisintegrations for Various Spectra	4-3

TABLES

Table		Page
1-1	Characteristics of Chambers Used for Previous Intercomparison Investigations	1-2
2-1	Chamber Description	2-8
3-1	Photochemical Test Calculated Parameter Definitions	3-2
3-2	Effects by Material	3-6
3-3	Ozone Half-Life Study	3-11
4-1	"Mylar/Teflon" Spectral Effect	4-2

Section 1
INTRODUCTION

Chambers in which systematic studies can be made of the reactions between hydrocarbons and nitrogen oxide in the presence of simulated sunlight have been in use for some twenty years. Such chambers have generally been successful in simulating the gross features of photochemical smog, such as production of oxidants and eye irritants, and haze. Intercomparison of the results obtained in these smog chambers has not been extensively attempted until relatively recently (Ref. 1), at which time the interest in individual hydrocarbon reactivity measurements led to an understanding of the need to compare the various facilities. Intensive comparisons of results obtained in eleven smog chambers have been performed by the Coordinating Research Council project CAPI-6, Techniques for Irradiation Chamber Studies, and CAPA 1-69 (Factors Affecting Reactions in Environmental Chambers). The range of physical characteristics of these chambers is shown in Table 1-1. A group of round-robin tests was conducted using these chambers as follows: (1) irradiation of seven different hydrocarbons with nitrogen oxide; (2) replicate runs to establish reproducibility using the propylene-nitrogen oxide system; (3) a reactant concentration study in which 3.0 ppm propylene was reacted with 3.0, 1.5, and 0.5 ppm nitrogen oxides (Ref. 2).

The differences observed among the chambers could not be accounted for analytically, and an experimental study of how various design and operational variables affect the photochemical reactions observed in smog chambers was instituted. This is a report of the results of this study, which are also the first reported results for a smog chamber illuminated by a xenon arc lamp. The facility was developed and initial tests performed under Phase I of the project, which has been previously reported (Ref. 3). Additional experimental and analytical work is in progress (see Section 5.1) and will be reported upon shortly.

Table 1-1

CHARACTERISTICS OF CHAMBERS USED FOR PREVIOUS INTERCOMPARISON INVESTIGATIONS

Volume (ft^3)	2.9 to 1140
Surface/Volume Ratio (ft^{-1})	0.78 to 4.91
Surface Type as S/V	
Stainless Steel	0 to 2.44
Aluminum	0 to 0.92
Glass	0 to 2.81
Plastic Film	0 to 0.83
Light Intensity (k_d, min^{-1})	0.16 to 0.40
Type of Lighting	Fluorescent lamp combinations, of sunlamps, black lamps, and blue lamps (both internal and external)

Section 2
EXPERIMENTAL METHOD

2.1 TEST CONDITIONS

The following combinations of factors have been studied in a full factorial test plan:

Materials	S/V	Spectrum	Cleaning
Aluminum	2.7 ft^{-1}	Full	Vacuum Off-gas
Pyrex	1.3 ft^{-1}	Cutoff	Purge at 110° F
Teflon			
Stainless Steel			

The testing sequence consisted of performing the photochemical tests for the aluminum surfaces, followed by Pyrex, Teflon, stainless steel, and a retest of the aluminum. This has allowed an analysis for time trend, to see if a systematic drift was present in the experiment. A number of replicate tests were performed. These were distributed among immediate replicates, replicates with 1 to 15 intervening runs, and the aluminum re-test replicates, which had greater than 50 intervening runs.

The propylene/NO_x system was used for all tests, at 3.0 ppm propylene and 1.5 ppm NO_x. The initial NO_2 content was nominally held at 10 percent. The chamber was held at 95 ± 3° F throughout all tests. Relative humidity was 25 ± 5 percent (49 to 59° F dew point). Chamber pressure was slightly above atmospheric (0.1 in. H_2O). Zero air was used to maintain chamber pressure, to make up for sampling and leakage, at about 3 percent/hour make-up rate.

2.2 APPARATUS

The apparatus used was specifically designed to meet the objectives of the study by allowing independent variation in materials configuration, lighting conditions, and cleaning technique. The illuminator produces a collimated light beam. Plates of materials can be placed parallel to the beam axis without affecting the light conditions. This decoupling of light and materials allows independent variation of the two factors. Major apparatus items are the smog chamber, the xenon arc lamp illuminator, the thermal enclosure for the chamber, and the gas analysis instrumentation.

2.2.1 Irradiation Chamber

The irradiation chamber is hexagonal in cross section, measuring 54 in. across the diagonal of the cross section. The chamber configuration is shown in Fig. 2-1 and the chamber support stand is shown in Fig. 2-2. Figure 2-3 represents a pictorial view of the chamber. The chamber is constructed of six flat side panels that fit into an extruded aluminum framework. The aluminum framework is coated with 5 to 8 mils of FEP Teflon. The resultant panels are bolted together and are supported from circular rings on the stand.

The faces of the chamber are of tempered 1/4 in. Pyrex glass to admit the light and pass the beam through the chamber with minimal reflection or absorption. The flat sides of the chamber are also fabricated from 1/4 in. tempered Pyrex glass. The working stress of the tempered Pyrex is 3600 psi, which results in an allowable pressure differential of 7.1 in. of water. This is based on the hexagonal faces, which are the weakest members. Sealing of the 1/4 in. Pyrex to the aluminum extrusion is accomplished with silicon rubber gaskets that have been off-gassed at about 10^{-5} torr for over 24 hours. The gasket is fitted between the aluminum channel and the Pyrex, and the Pyrex is pressed into a channel section in the extrusion. A silicon rubber O-ring is used to seal adjacent aluminum extrusions which are bolted together. Additional sealing is accomplished with a coat of Dow Corning 30-121 RTV silicon rubber on all external joints.

Three 1-in. diameter ports are located in one of the lower side panels. The ports are fabricated from brass and are coated with FEP Teflon. Sealing of these ports to the Pyrex chamber walls is accomplished with silicon rubber gaskets. Sealing of tubes inserted into the ports is accomplished with Teflon seals. Tubes can be fitted into these ports and adjusted to various distances into the hexagon. The rear port is used for a gas thermocouple, which is Teflon coated and shielded from direct illuminator radiation. The front port has a 1-in. diameter Pyrex tube installed that is used for venting the chamber.

The center port is used for gas sampling. A 1-in. diameter Pyrex tube containing a concentric 7-mm tube is used. The sample enters at about the geometric center of the chamber, and is drawn to a sample manifold through a 1/4-in. Teflon tube, and thence to the analysis instrumentation. The sample contacts only Pyrex or Teflon before entering the instruments. Delay time from sample withdrawal to instrument inlet is about 1-1/2 min.

A cleanout port is located in this same Pyrex panel. This port is 3-in. diameter and is used for chamber outgassing during vacuum off-gas cleaning. A Pyrex disc with a silicon rubber gasket is used to seal this port during normal operation. Metallic parts are all coated with FEP Teflon. A Pyrex relief valve is also mounted on this panel. This relief valve has a 2-in. diameter opening leading to the chamber. The valve utilizes a water seal principle and the relief setting is adjusted by the addition or withdrawal of water. Both negative and positive differential pressure protection are provided. An overflow trap is included to prevent water from entering the chamber.

A side stream mixer is also located on this panel. This mixer consists of a 6-in. diameter duct connected to the panel at a point 1/3 of the way from the front and 1/3 of the way from the rear of the chamber. Gas is circulated through the duct by means of a Teflon-coated fan blade installed in the duct. The blade is connected to a shaft that penetrates the duct through a rotary Teflon seal. The shaft is connected to a motor via a pulley and belt which are located outside the chamber. The fan is rotated

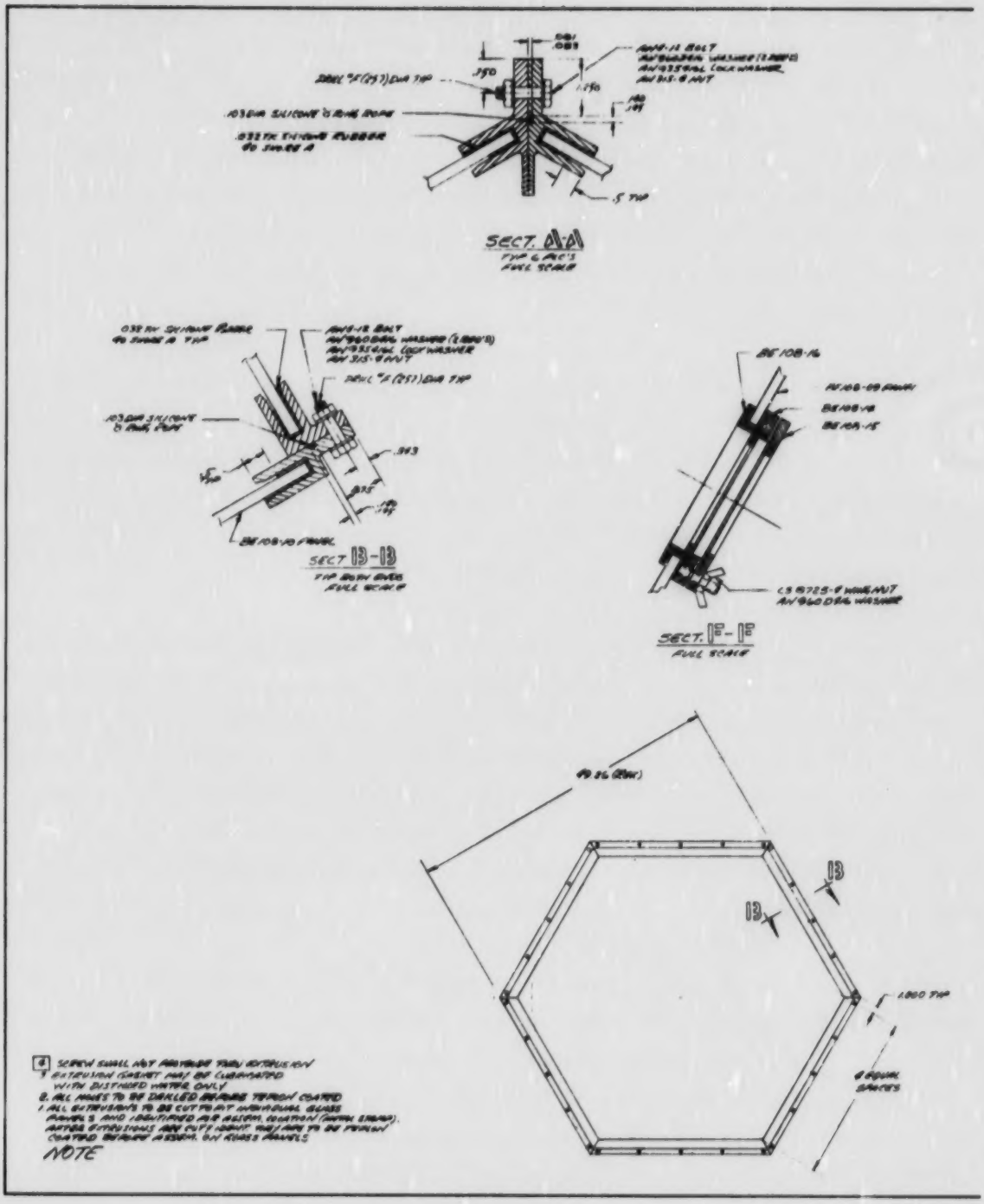

Fig. 2-1 Smog Chamber Assembly

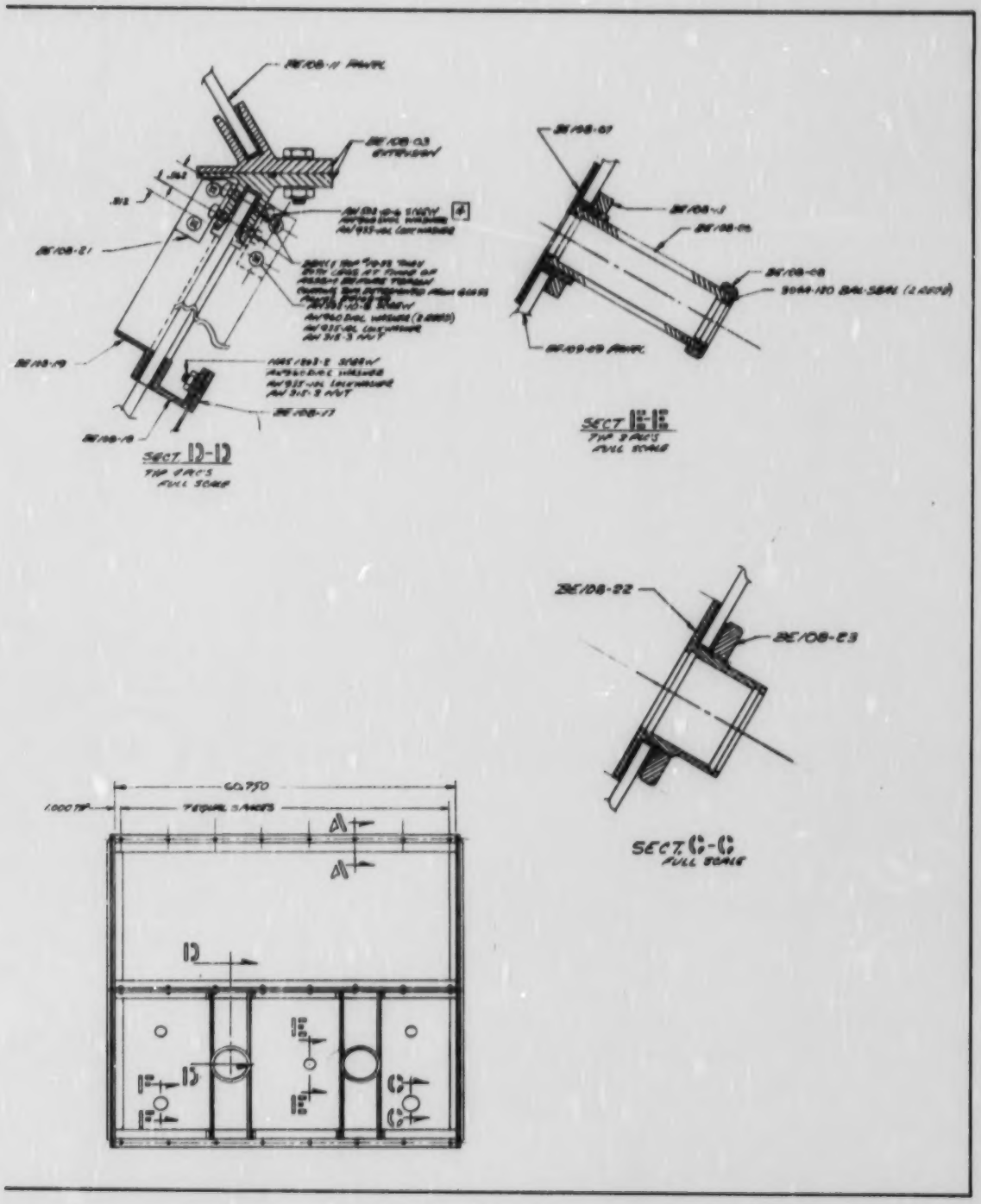

Fig. 2-1 Smog Chamber Assembly (Cont.)

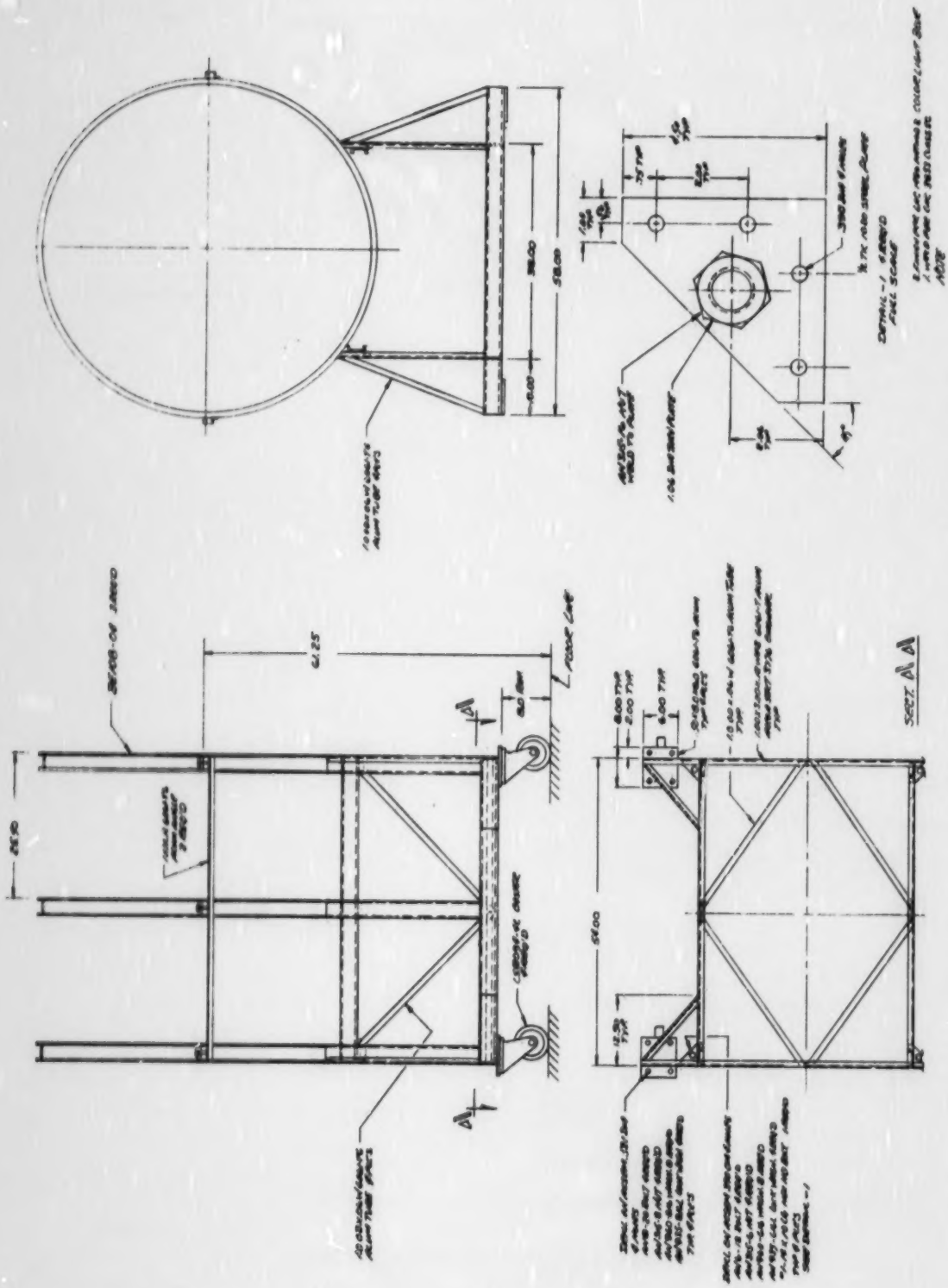

Fig. 2-2 Stand Assembly

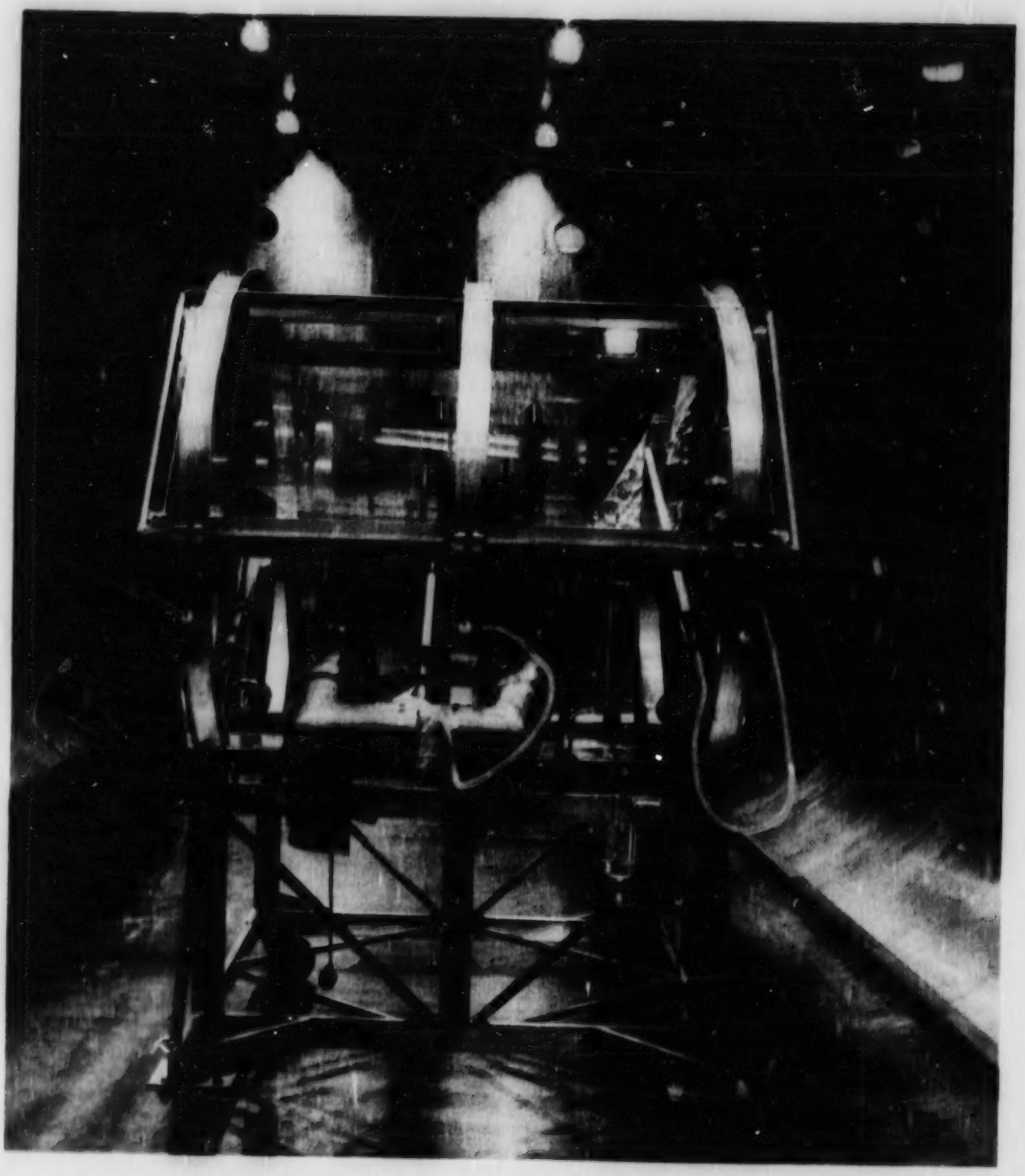

Fig. 2-3 Environmental Chamber Showing Side Stream Mixer, Charge Ports, and Clean-Out Port

at 250 rpm, producing a circulation rate of approximately 75 cfm. The inlet end of the duct enters the chamber at a 45-deg angle to minimize short circuiting of the gas circulation. All parts of the side stream recirculator are coated with Teflon. The mixer is operated during charging of the chamber only. It is shut off during photochemical tests.

The chamber is mounted at each hexagonal apex to a circular structural framework, which in turn mounts to a dolly with casters for easy transport of the chamber. The structural frame is configured to allow chamber assembly within the framework. A locating jack system is used to adjust the height of the chamber to exactly match the height of the light source.

Geometric characteristics of the chamber are summarized in Table 2-1.

Table 2-1

CHAMBER DESCRIPTION

Configuration	Hexagonal Prism
Length	60 in.
Diagonal	54 in.
Volume	65.9 ft^3
Surface Area	
End Plates	26.4 ft^2
Side Plates	67.5 ft^2
Total	93.9 ft^2
S/V	1.43 ft^{-1}

2.2.2 Illuminator

The irradiation source for the chamber is external to the chamber. This external source consists of an arc lamp situated in front of a large parabolic reflector.

Collimated energy from the reflector is directed toward the chamber. The collimated beam used as the light source for the irradiation chamber is 5 ft in diameter. The light source for the illumination system is an air cooled Osram compact xenon arc lamp (6,500 watt nominal rating). The fireball for the lamp is 2.4 by 9 mm. The optical system consists of a 5-ft diameter parabolic primary mirror and a spherical back-collector mirror. The primary mirror is made of copper with a rhodium plating with vacuum deposited aluminum over the rhodium. An SiO coating is used to protect the aluminum. Reflectance is approximately 0.9 at a wavelength of 300 nm. The spherical back reflector is similarly coated. The back reflector is utilized to capture energy from the lamp that would normally not strike the parabola, and focus it back on the parabolic reflector. The optical system collects about 35 percent of the lamp radiated light and directs it as a collimated beam into the chamber front face. The lampholder casts a shadow about 1.5 ft^2 in area, which obscures about 8 percent of the beam. This shadowed area has no appreciable effect on the experimental data.

For the cut spectrum configuration, a plane reflector is mounted behind the chamber rear face. This reflector provides a second pass of the light through the chamber. It is a front-surfaced, aluminized SiO_x-coated reflector, to maintain reflection down to 300 nm wavelength.

The illuminator is integrated into a searchlight housing. The housing is on casters, which allows the illuminator to be moved readily.

2.2.3 Thermal Enclosure

A thermal enclosure is used to control the chamber temperature during a photochemical run. Design requirements for the thermal enclosure are maintenance of chamber gas temperature at 95 ± 3° F. The enclosure, depicted pictorally in Fig. 2-4 with the chamber installed, consists of a plywood housing insulated with fiberglass, with heated air circulating throughout the enclosure. The enclosure has a hexagonal-shaped hole in the rear to allow the chamber to protrude. The front end of the thermal enclosure

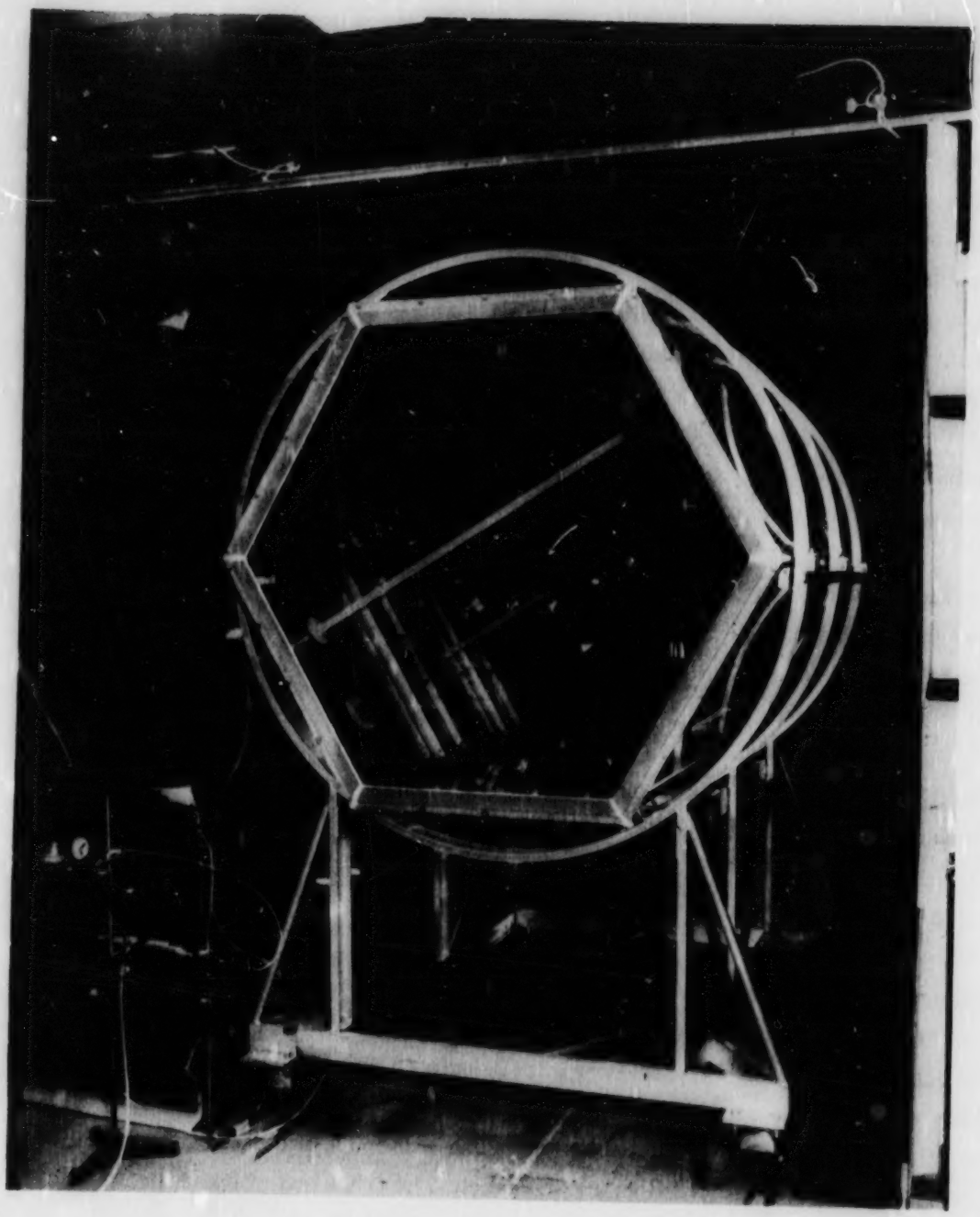

Fig. 2-4 Chamber Inside Thermal Enclosure

has sliding doors that allow easy removal and installation of the chamber. These doors also have a hexagonal-shaped hole that will allow the forward end of the irradiation chamber to protrude. This allows the illuminator energy to enter the chamber. Both the rear and forward hexagonal openings in the enclosure fit tightly to the chamber to minimize gas leakage from the enclosure. The interior surfaces of the enclosure are insulated with 3 in. of fiberglass.

A centrifugal blower is utilized to circulate approximately 1500 cfm of air over four 1.3-kw heaters that are used for thermal control. Three of the heaters are manually switched on or off and the fourth heater is thermostatically controlled to maintain the enclosure air temperature at a fixed level. This system allows use of the fixed heaters for purge cleaning, or warm-up, and coarse temperature control, with fine temperature control being accomplished with the thermostatically controlled heater. The thermal sensor is a West resistance bulb controller. This controls the air temperature in the thermal enclosure. Air circulation is accomplished with a centrifugal blower that passes air through plenums located at the bottom of the thermal enclosure. The heaters are located in these plenums. Air passes out of the plenums, over the chamber and is withdrawn out of the top of the thermal enclosure, where it is recirculated to the heater plenum. The thermal enclosure is approximately 8 ft high by 8 ft wide by 6 ft long.

2.2.4 Material and S/V Changes

Plates of the material under study are inserted into the chamber, oriented parallel to the light-beam axis of collimation, and vertically. These plates vary from 5-3/8 to 22-3/8 in. in width and are the height of the chamber. Plates are arranged in six sets, with each set running the length of the chamber. Frequent open spaces interrupt each set of plates, and form openings that are the height of the chamber and 2 to 4-1/2 in. wide, to allow the sampling and vent tubes to penetrate into the chamber, and to promote mixing of the entire chamber contents. Figure 2-5 gives the plate layout. Either six or three sets of plates are used, which gives either 2.7 or 1.3 ft^{-1}

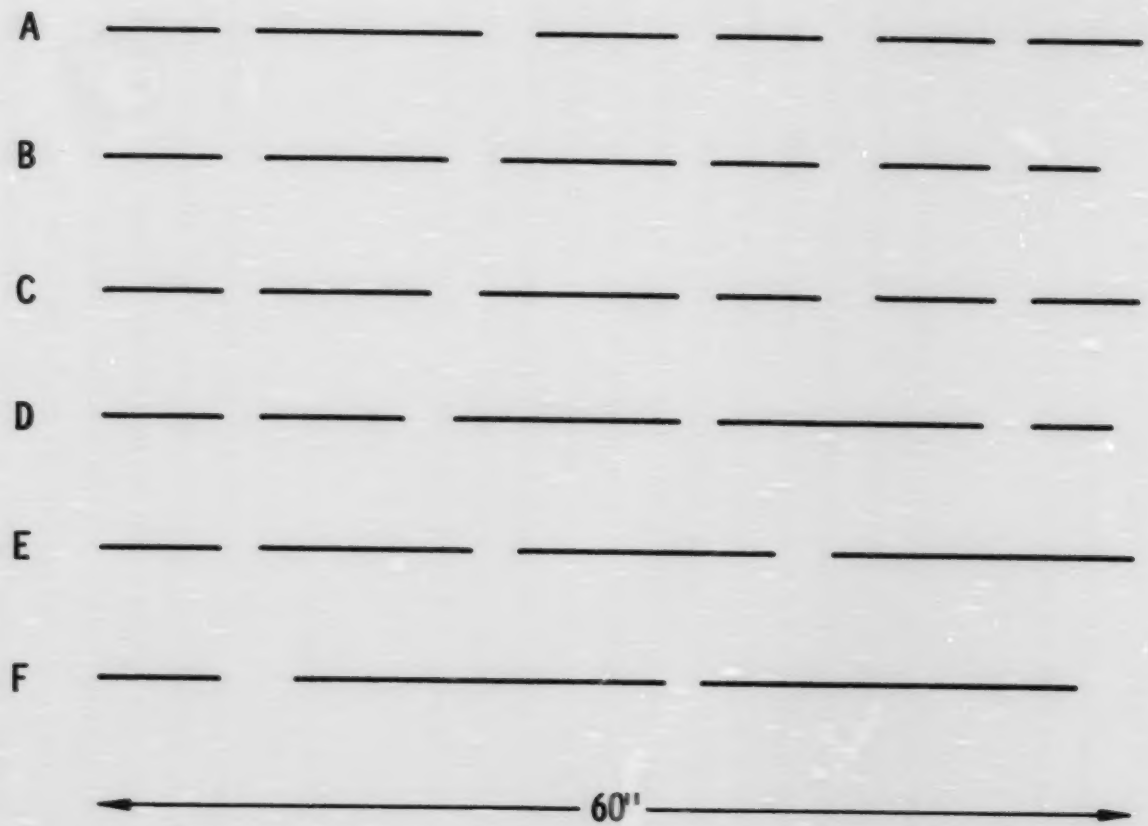

NOTE: Plate sets B, C, E removed for low S/V configuration.

Fig. 2-5 Arrangement of Surface Plates

of the material under study. The metallic materials are polished to a mirror finish. The materials details are aluminum – 1100 H 14 alloy, stainless steel – type 304, Pyrex-Corning 7740 plates, and Teflon – 5 mil FEP film.

2.2.5 Spectral Distribution and Spectral Changes

The spectral interval of interest in atmospheric photochemical simulation is 300 to about 400 nm. The lower wavelength is the natural cutoff provided by the earth's ozone layer, and the upper wavelength is set by the energy required to dissociate NO_2. It is generally recognized that compact xenon arc lamps provide the best available match for this UV region.

Two spectral distributions were used in these experiments. The full spectrum configuration is shown in Fig. 2-6. The second distribution is the cutoff spectrum, and is also shown in the figure. This is obtained by placing a sheet of 3/16 in. thick Plexiglas between the light source and the smog chamber. To avoid aging effects, a fresh sheet of Plexiglas is used after about each fifth test. Total light intensity is restored to the same value as used for the full spectrum runs by providing a second pass of the light through the chamber. The front surfaced aluminized reflector is used for this purpose.

Spectral data were taken with an Optronics Laboratory spectroradiometer. The radiometer consists of a calibrated photovoltaic cell, a grating prism spectrometer, and blocking filters. Digital readout is provided over a range of 10^{-9} to 10^{-2} watt/cm^2-nm. Bandpass is 5 nm. The unit is calibrated against an NBS standard quartz iodide lamp, over the wavelength interval of 250 to 1100 nm. Note that the characteristic xenon arc lamp peak at 467 nm is easily seen by the radiometer. These data are in agreement with earlier data taken using a photomultiplier tube spectroradiometer unit.

Measurements of the light beam were made at the plane corresponding to the front window of the chamber, and of the beam at the exit of the chamber, after passing

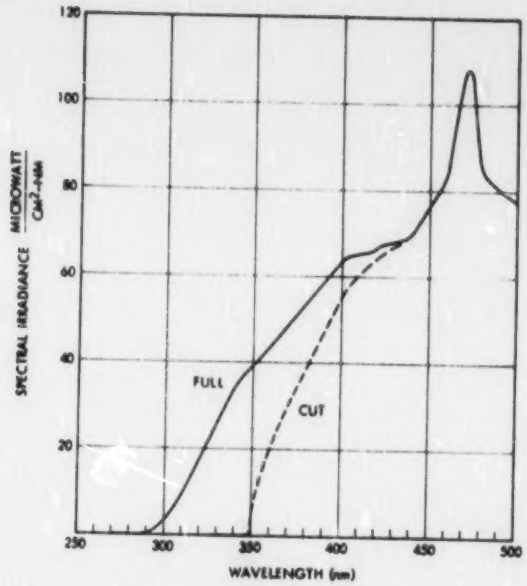

Fig. 2-6 Measured Spectral Irradiance Inside LMSC Smog Chamber – Full and Cut Spectra

through the front and rear 1/4-in. Pyrex window. To measure spectral irradiance inside the chamber, the rear window is removed, and the spectroradiometer entrance slit positioned somewhat inside the chamber. These are the values shown in Fig. 2-6.

Total light intensity has been maintained at k_d of 0.3 min^{-1} throughout the test series.* To measure k_d the smog chamber is filled with pure N_2 (< 100 ppm O_2, < 0.1 ppm HC) and about 1.5 ppm NO_2 added. The lamp is turned on, allowed to stabilize, and the chamber illuminated for three or four successive one-minute intervals. The data are plotted on semi-log paper and usually show the expected upward deviation from linearity after the third one-minute interval. Two or three NO_2 instruments are used for each k_d determination, and usually agree within 10 percent. Measurements of k_d are performed each time a new S/V configuration is established. Figure 2-7 shows a typical plot.

*Lamp power was adjusted to maintain k_d at a constant value throughout the study. A variation of perhaps ±10 percent occurred due to uncompensated aging effects of the lamp, reflector, and filter.

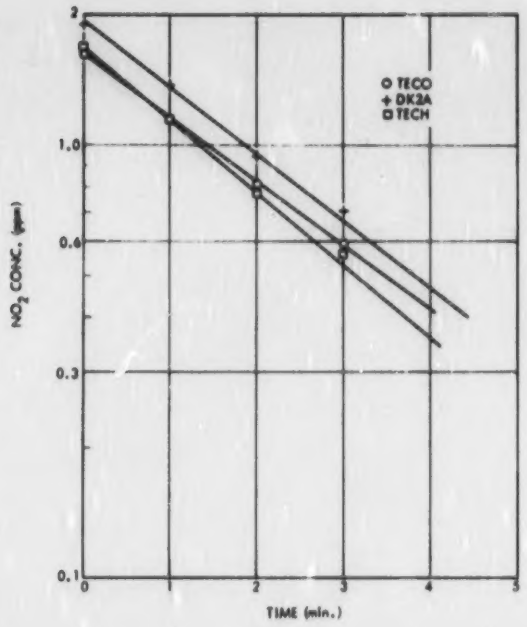

Fig. 2-7 Typical Raw Data for Determining k_d

2.2.6 Cleaning Technique

The two cleaning techniques used are: purging at 110° F, or vacuum off-gassing. Purge cleaning consists of holding the chamber overnight at a temperature of 110 ± 3° F while 4 to 6 chamber volumes of pure air are purged through the chamber. For vacuum off-gassing, the smog chamber is moved to an adjoining 18 by 18 by 36-ft vacuum chamber. The vacuum chamber is pumped by Roots Blowers and mechanical pumps which prevents any back migration of pump oil. The chamber walls are 304 stainless steel, polished to a No. 4 mill finish. The smog chamber is held at about 2 microns pressure (or less) for at least 16 hours. During this time, the chamber is maintained at about 100° F. After the off-gassing, the smog chamber is repressurized by bleeding charge gas into the smog chamber while repressurizing the vacuum chamber. Figure 2-8 shows the smog chamber inside the vacuum chamber.

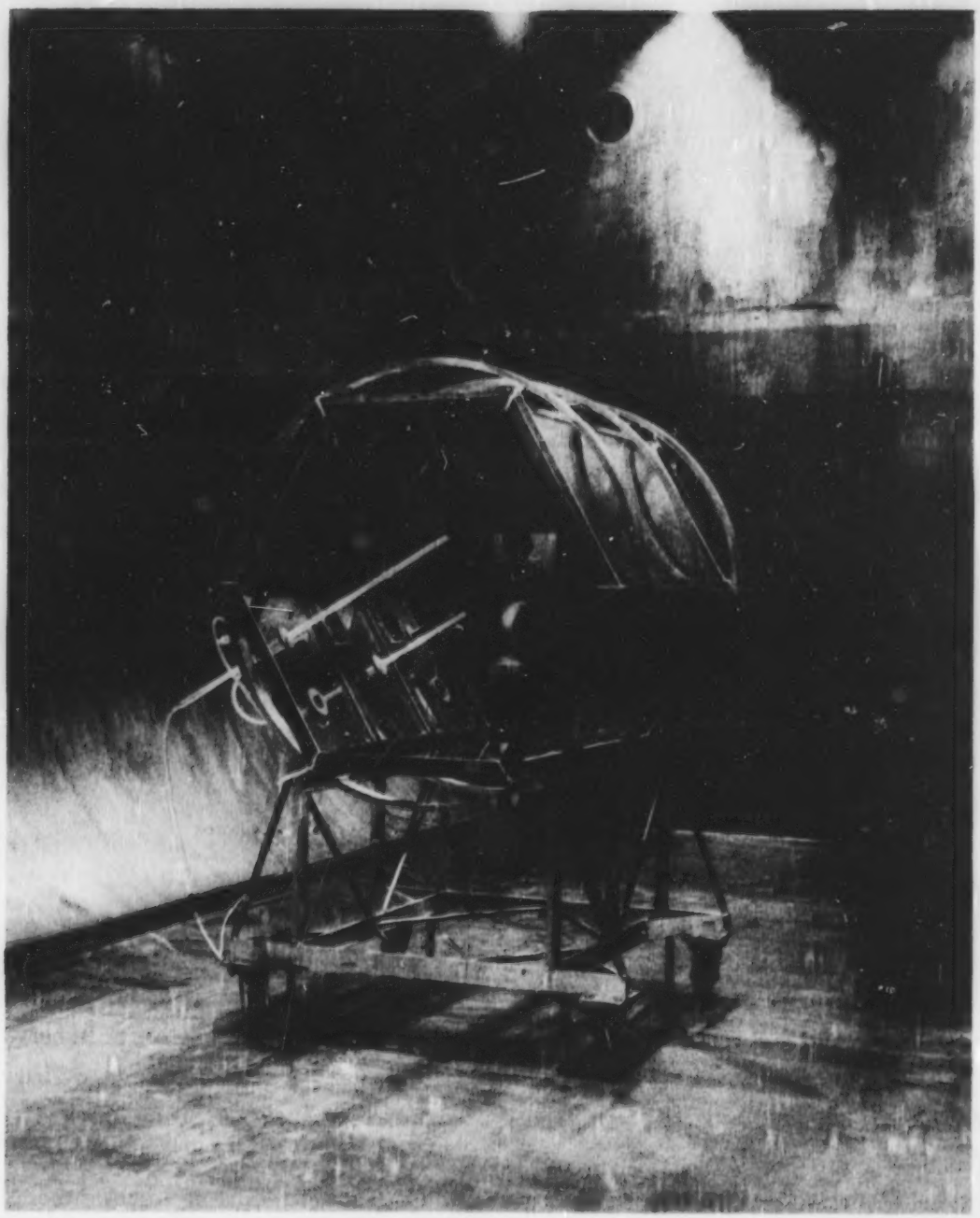

Fig. 2-8 Smog Chamber During Vacuum Off-Gassing Cleaning

2.2.7 Chamber Charging Technique

The chamber is charged with synthetic compressed air. The air is purchased from a single vendor to a specification of < 0.1 ppm total hydrocarbons (as methane), and < 10 ppm hydrogen. The air is produced by combining nitrogen gasified from liquid nitrogen and electrolytic oxygen. The oxygen is made by electrolysis of distilled water. It then is further purified by catalytic combustion of the trace hydrogen, followed by molecular-sieve drying of the oxygen. A pre-charge determination of total hydrocarbons verifies the air purity. The chamber is charged through a stainless steel humidifier, packed with Rashig rings and filled with triple distilled water. Starting dew point is adjusted to 54 ± 5° F by dilution with the dry pure air.

Reactants are added to the chamber from stock cylinders of about 350 ppm in nitrogen. The reactant blends are transferred using separate 1/2 liter sampling cylinders. The transfer cylinder is pressurized at about 200 psi, placed in the charge manifold, and slowly bled to the smog chamber. In this technique, the transfer cylinder pressure (which is read to 0.5 psi) becomes the reproducibility limit for the initial reactant charge.

2.3 CHEMICAL ANALYSIS METHODOLOGY

2.3.1 NO_2-NO_x

Nitrogen dioxide is monitored by the modified Saltzman-Lyskow wet chemical technique, utilizing a continuous sampling Technicon Autoanalyzer unit. The NO_2 absorbing solution is made from 2.0-gm N-1-naphthylethylenediamine dihydrochloride, 100-gm sulfanilic acid, 5-cc Kodak Photoflo, and 1 liter glacial acetic acid in 5 gallons of water. The lifetime of the solution is greater than 1 month when stored in an aluminum foil covered bottle and shielded from air exposure. The gas sampling system consists of two 15-cm by 2.4-mm I.D. (28 turn) glass mixing coils in series where the gas sample stream contacts the absorbing solution, an accumulator/liquid-gas separator,

a flowmeter to measure sampling rate, a chain driven peristaltic pump using variable flow fluoroelastomer tubes, a colorimeter with a 50-mm flow cell, and an extended range recorder. Gas sampling rate is 150 cc/min and liquid sampling rate is 1.5 cc/min.

When new absorbing solution is prepared, a static calibration using $NaNO_2$ solutions ranging from 1.5×10^{-3} to 1.5×10^{-1} μl NO_2/ml is performed. NO_2 gas concentrations are determined from the formula

$$\text{pphm } NO_2 = \frac{(A)\ (B)}{(C)\ (D)}\ 100$$

where:

A = microliters NO_2 gas per milliliter of liquid standards

$$= \frac{(\text{mg/liter } NaNO_2)}{(\text{Mol wt. } NaNO_2)} \quad \frac{(24.5 \text{ liters/mole})}{0.72 \text{ moles } NaNO_2/\text{mole } NO_2}$$

where 24.5 is the molar volume at 25° C and 760 torr and 0.72 is the Saltzman factor

B = flow rate of absorbing solution reagent (ml/min)

C = gas stream flow rate (liters/min)

D = column efficiency (expressed decimally)

Daily dynamic calibrations are performed using standard Metronics 4-cm constant rate NO_2 permeation tube. The permeation tube is placed inside a constant-temperature condenser. Low NO_2 concentrations are obtained by passing compressed air through a calibrated flow meter and then sweeping the NO_2 from the permeation tube into a 12.5 liter dilution flask. The NO_2 stream enters the bottom of the flask and sampling is done at the top using a single 4-way path to the gas stream. The dilution flask pressure is measured with a -0.5 to +0.5 in. water Magnihelic gage and is adjusted with a vent line constriction to get pressure resembling chamber run conditions (+0.02 in. H_2O). The dilution system is all Teflon and glass except for small Tygon connections.

Permeation tube NO_2 concentrations are determined from the formula

$$C = \frac{(L)\,(K)\,(P_t)}{F} \times 100$$

where:

- C = gas concentration (pphm)
- L = length of permeation tube (cm)
- K = molar volume/molecular weight = 0.532 for NO_2 at 25° C and 760 torr (liter/gm)
- P_t = permeation rate of NO_2 at temperature t (ng/min per cm of tube length)
- F = carrier gas flow rate past tube (cm^3/min)

Nitric oxide is continuously measured with a Thermo Electron Corporation Model 12A chemiluminescent gas monitor and Honeywell 18 recorder. This instrument measures the chemiluminescent reaction of NO and O_3. Gas flow to the instrument is 150 cc/min. The NO_x mode of the instrument uses a stainless steel converter run at 800° C to reduce NO_2 to measurable NO. Converter efficiency has been established at 99+ percent. Instrument zero, full scale and photomultiplier tube dark current are checked prior to turning on the O_3 generator. The instrument is calibrated daily by the dynamic NO_2 dilution gases and by a stock 88 ppm NO in N_2 standard gas. Linearity of the instrument is periodically confirmed by the exponential dilution technique. Precision is within 5 percent. Figure 2-9 shows an exponential dilution linearity check.

2.3.2 Ozone

Ozone is measured directly and continuously by a McMillan Model 1100 Ozone Meter. This instrument measures the chemiluminescent reaction of ozone and ethylene. The meter has four scales, with 0 to 2 ppm scale most commonly used. Daily meter calibration is done at 1 ppm before and after a photochemical run by using a McMillan 1000 ozone generator. The output of the generator is regulated by sliding cover for the UV lamp and output at 1.00 ppm (999 dial setting) is checked with a null meter. Periodic

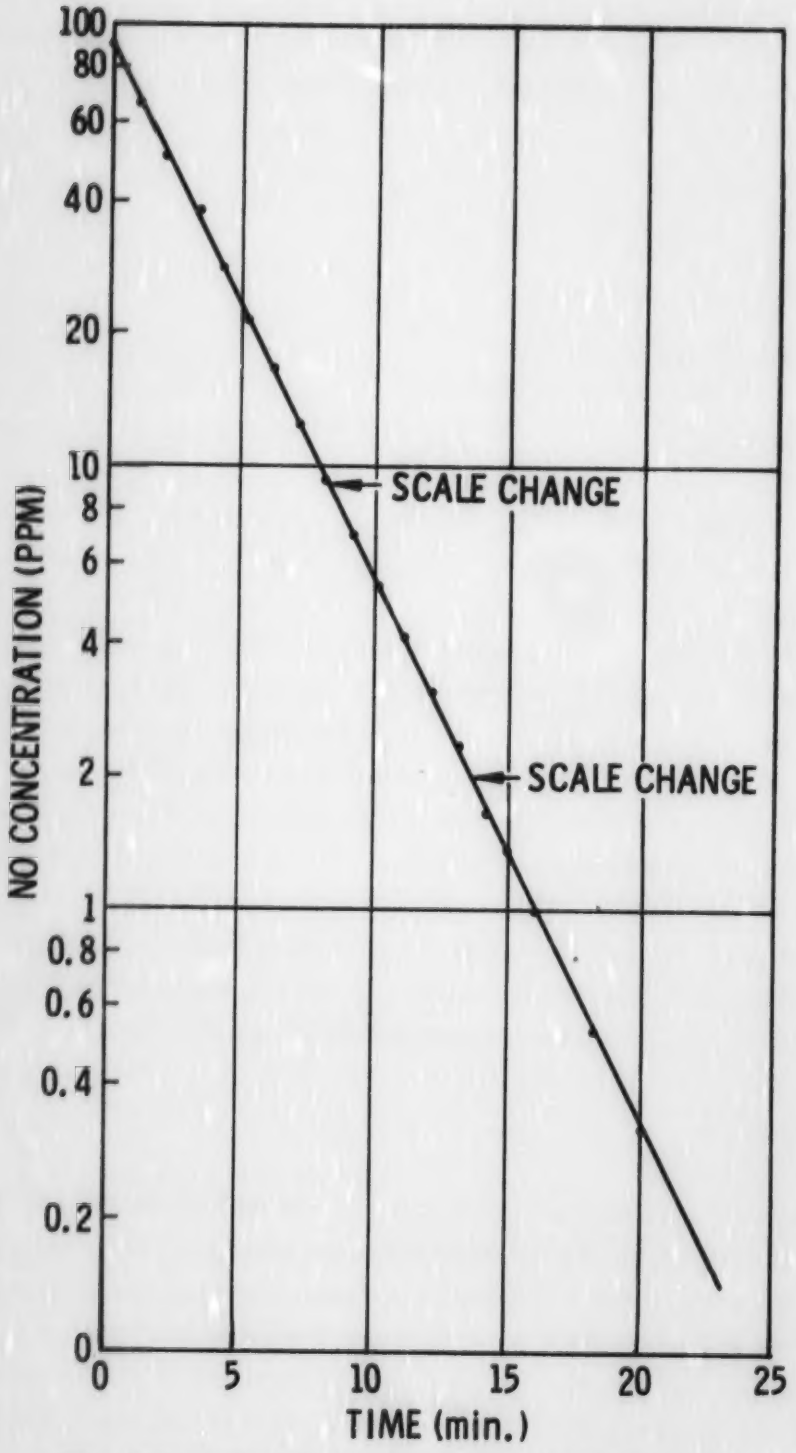

Fig. 2-9 Typical Linearity Check of NO Instrument

calibrations of the generator and meter are done with the neutral buffered KI technique. The 2-percent KI absorbing solution is calibrated with a stock I_2 solution titrated against standard $Na_2S_2O_3$. The absorbance of the resulting KI/I_2 solution is measured on a Perkin-Elmer 202 spectrometer at 350 nm. Precision is about 4 percent. In the first 20 months of usage of the ozone generator, the calibrations against neutral KI showed no significant drift (< 5%). The null meter-front panel adjustment potentiometer technique, which is used to maintain the ozone generating lamp light output, was evidently effective. At that time the generator malfunctioned and was returned for repair and recalibration. The good stability observed may also reflect the constant air flow system and the air pre-treatment. Room air is filtered through an MSA Type N canister and a pre-ozonation UV lamp. This lamp produces ozone which converts trace NO to NO_2. The air then goes through a molecular sieve 13X filter which destroys the ozone. This scheme avoids loss of part of the calibrated ozone output by the $NO-O_3$ reaction.

Ozone concentration is corrected by checking 1.00 ppm before and after a run. If a discrepancy is noted, the initial and final readings at 1 ppm from the generator are plotted linearly against time. Corrections are read from the line and applied to the readings. Corrections are applied if the meter is more than 5 percent different from the generator. The largest drift noted was about 18 percent.

2.3.3 Total Hydrocarbons

Chamber total hydrocarbons as CH_4 are monitored with a F&M Model 700 gas chromatograph with a Model 810 electrometer using an O_2-H_2 flame ionization detector and an unpacked 1/8 in. O.D. stainless steel column. Calibration is done from a zero air cylinder with a THC concentration of 0.07 ± 0.03 CH_4. The cylinder concentration was determined at the supplier and checked upon delivery. Chamber samples from the glass manifold are drawn through a 1/8 in. O.D. Teflon line and then through a sliding sampling valve by a small vacuum pump.

2.3.4 Propylene

Propylene is measured using the same detector and valve used for total hydrocarbons. A Carle Microvolume Switching Valve is used for analysis selection. The column for propylene is 0.6 ft × 1/8 in. 100/120 mesh Porapak S stainless steel. The oven temperature is 105°C; the detector is set at 150°; and the injection port is set at 125°. The sampling loop has a 5.0 cc volume, which gives an LLD of 0.03 ppm.

Calibration was done using a stock cylinder. The concentration and linearity from 0.05 to 3.00 ppm of the analysis were confirmed. Precision at 3.00 ppm is less than 5 percent.

2.3.5 Acetaldehyde

Acetaldehyde uses the other detector of Model 700 gas chromatograph and a separate Model 810 electrometer. The column is a 20-percent FFAP Chromosorb W (DMSC treated), 60/80 mesh, 20 ft × 1/8 in. stainless steel column. The 10.0 cc sampling loop and valve use the same Teflon line from the manifold and vacuum pump as do the propylene and total hydrocarbon analyses. Oven, detector, and injection port temperatures are the same as for propylene. Calibration is done with a stock cylinder and linearity has been established from 0.08 to 1.50 ppm, with an LLD of 0.03 ppm and precision less than 10 percent at 1.50 ppm. When the column is too noisy to give useful data, the Porapak S column used for propylene can be used for acetaldehyde analysis, although the acetaldehyde peak is broad and LLD is 0.07 ppm. A comparison of acetaldehyde concentration indicated by both columns shows quite good agreement.

2.3.6 Peroxyacetyl Nitrate (PAN)

Peroxyacetyl nitrate is measured on a Varian Model 600C gas chromatograph using a tritium electron capture detector with an N_2 carrier and a 5-percent Carbowax 600 on 60/100 mesh Chromosorb W (DMSC treated) 22 in. × 1/8 in. Teflon column run at ambient temperature (25°C). The 0.5 cc sampling loop is made of Teflon and gives

an LLD of about 0.003 ppm PAN. Standards are prepared by irradiation of an ethyl nitrate-oxygen mixture with a UV lamp. Concentration of PAN in this standard is determined by infrared analysis, and the 10 cm cell containing the mixture is purged into a Tedlar bag with air measured by a wet test meter. Extensive calibration has shown good linearity from 0.05 to 1.0 ppm with precision estimated at 25 percent.

2.3.7 Moisture (Water)

Moisture content was monitored with a Cambridge System Model 992 Hygrometer. Samples were drawn periodically from the chamber manifold through a two-way sampling valve. Otherwise, room air was purged through the instrument allowing continuous instrument readout. Stable instrument response at 250 cc/min sample flow was less than 3 minutes for dew points ranging from 48° F to 56° F. Precision was less than 0.1 percent, based on saturation pressure.

Section 3
RESULTS

Behavior of photochemical reaction systems is usually characterized by a few chosen calculated parameters. In this work, the parameters used are those defined by the CAPI-6-69 Project, with the addition of several measures that appear interesting, for a total of 23, as defined in Table 3-1.

Parameter (17) was added to describe the NO disappearance as good NO data are available from the chemiluminescent instrument. For almost all runs, parameter (17) is smaller than parameter (1), the NO_2 formation rate.

An induction period of several minutes is observed when the chamber lights are turned on. During this period, the NO disappears slowly, whereas the NO_2 is increasing (after accounting for the instrument lag time). Such an induction period would make parameter (17) smaller than parameter (1). Further analysis of this behavior and of the ratio of NO_2 at maximum to initial NO_x will be conducted and reported upon in the Phase III report. The NO/NO_2 rate difference is largest for the stainless steel surfaces.

Parameters (18) and (19) are calculated to give additional insight into the NO_2 and oxidant dosage values, by normalizing them to a potential maximum dosage represented by the denominator.

Parameter (20) describes the NO_2 curve to some extent, by giving the full width at half maximum of the curve. It has been included to facilitate comparisons of the NO_2 curve shape on a numerical basis.

Parameters (21) to (23) give various defined intervals in the photochemical run. The crossover time is used because it is well demarked on the run graphs. Measuring time from the crossover time yields system behavior characteristics that are less dependent on initial conditions.

Table 3-1

PHOTOCHEMICAL TEST CALCULATED PARAMETER DEFINITIONS

NO_2 Formation

(1) Rate = $\frac{NO_i}{2T_{1/2}}$ where $T_{1/2}$ is the time to form an amount of NO_2 equal to 1/2 the initial NO in addition to the NO_2 present initially; and NO_i is the initial NO concentration in ppb (ppb/min)

(2) T_{max} = time, in minutes, to the maximum NO_2 concentration (min)

(3) Dose = $\int_0^{300} NO_2\, dt$ where NO_2 is NO_2 ppm and t = minutes (ppm-min)

Oxidant Formation

(4) Max. Rate = $\frac{\text{Max. Oxidant}}{2(T_{3/4} - T_{1/4})}$ where $T_{3/4}$ and $T_{1/4}$ are the times to form 3/4 and 1/4 the maximum oxidant; and max. oxidant is the maximum oxidant concentration (ppb/min)

(5) Avg. Rate = $\frac{\text{Max. Oxidant}}{2T_{1/2}}$ where $T_{1/2}$ is the time to form 1/2 the maximum oxidant, and Max. Oxidant is the maximum oxidant concentration (ppb/min)

(6) Max. Conc. = maximum oxidant concentration (ppm)

(7) T_{max} = time to the maximum oxidant concentration (min)

(8) Dose = $\int_0^{300}$ Oxid. dt where Oxid. is oxidant and t = minutes (ppm-min)

Hydrocarbon Disappearance

(9) Final Conc. = ppm hydrocarbon after 300 minutes irradiation (ppm)

(10) $T_{0.75}$, $T_{0.5}$ and $T_{0.25}$ = the times required to reduce the hydrocarbon concentration to 3/4, 1/2, and 1/4 of the original (min)

(11)

(12)

(13) Max. Rate = $\frac{HC_i - HC_f}{2(T_{3/4} - T_{1/4})}$ where $T_{3/4}$ and $T_{1/4}$ are times for the disappearance of 3/4 and 1/4, respectively, of the hydrocarbon disappearing in 300 minutes; HC_i is the initial hydrocarbon concentration; and HC_f is the final hydrocarbon concentration (ppb/min)

Table 3-1 (Cont.)

(14) Avg. Rate = $\frac{HC_i - HC_f}{2T_{1/2}}$ where $T_{1/2}$ is time for the disappearance of 1/2 the hydrocarbon disappearing in 300 minutes; HC_i is the initial hydrocarbon concentration; and HC_f is the final hydrocarbon concentration (ppb/min)

(15) Max. Ald. = Maximum total aldehyde concentration (acetaldehyde for these runs) (ppm)

(16) Max. PAN = Maximum peroxyacetylnitrate concentration (ppm)

(17) NO Rate = $\frac{NO_i}{2T_{1/2}}$ where NO_i = initial NO and $T_{1/2}$ = time to reduce NO to half of original concentration (ppb/min)

(18) NO_2 Dose Factor = $\frac{NO_2 \text{ Dose}}{300\ NO_{x_i}} \times 100$ where NO_{x_i} = initial NO_x (%)

(19) Ozone Dose Factor = $\frac{\text{Ozone Dose}}{300\ NO_{x_i}} \times 100$ (%)

(20) NO_2 FWHM = Full width at half-maximum of NO_2 curve (min)

(21) Crossover Time = Time at which NO and NO_2 curves cross (min)

(22) 2-21 = NO_2 T_{max} - Crossover time (min)

(23) 7-21 = Ozone T_{max} - Crossover time (min)

The four materials affect the behavior of the propylene/NO_x reaction system differently. As a summary, Figs. 3-1 to 3-4 show the photochemical results for Teflon, Pyrex, aluminum, and stainless steel, respectively. Each figure gives the average for the two S/V ratios and the two cleaning techniques for each spectral distribution. Run parameter data are given in Appendix A for each run.

Table 3-2 gives the effects of the three independent variables, for the four materials separately. Notations for that table are:

- m = mean value of the parameter
- A = effect of changing from low S/V value (1.3 ft^{-1}) (represented by -1) to high S/V value (represented by +1) (2.7 ft^{-1})
- B = effect of changing from cutoff spectrum (-) to full spectrum (+)
- C = effect of changing from purge cleaning technique (-) to vacuum offgassing (+) cleaning technique
- AB, AC, BC, ABC = interaction effects
- s = estimate of the standard deviation of replicates
- 10% = value of parameter that would be exceeded by chance 1 time in 10 if true value of effect were zero, i.e., significant at 10% level
- 1% = value of parameter that would be exceeded by chance 1 time in 100 if true value of effect were zero, i.e., significant at 1% level

The table is calculated using standard methods for factorial tests (Ref. 4). For each material, 2 levels of A × 2 levels of B × 2 levels of C = 8 runs are available. From these we form 4 pairs that differ only with respect to one of the independent variables (A, B, or C). The average of the four differences is then the estimated effect of the independent variable. This procedure is repeated three times. For this balanced experimental plan the estimated effects are uncorrelated with each other, a decided advantage in interpretation. Interactions are determined from the intereffects of the variables.

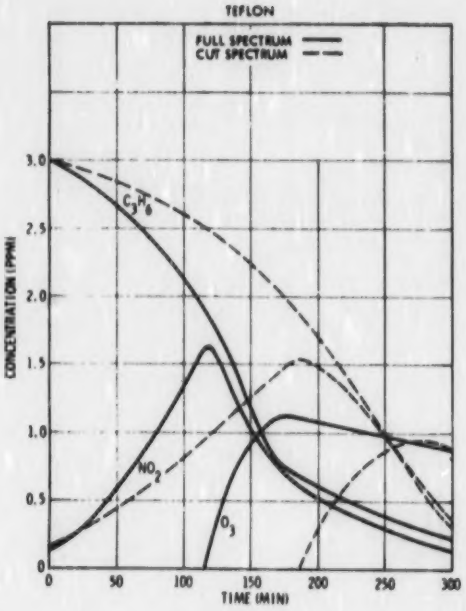

Fig. 3-1 Composite Photochemical Test Results for Teflon Film Surfaces

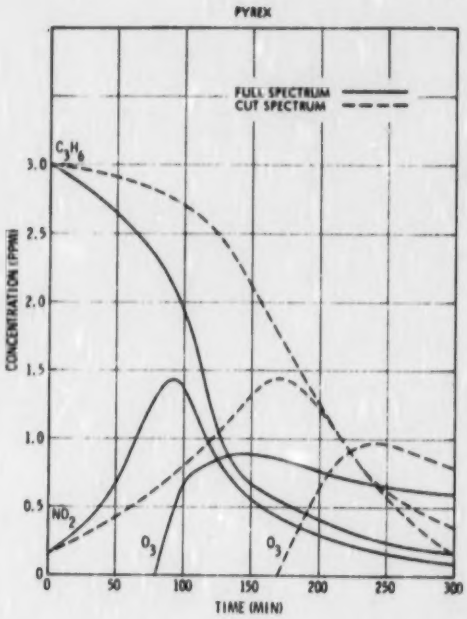

Fig. 3-2 Composite Photochemical Test Results for Pyrex Surfaces

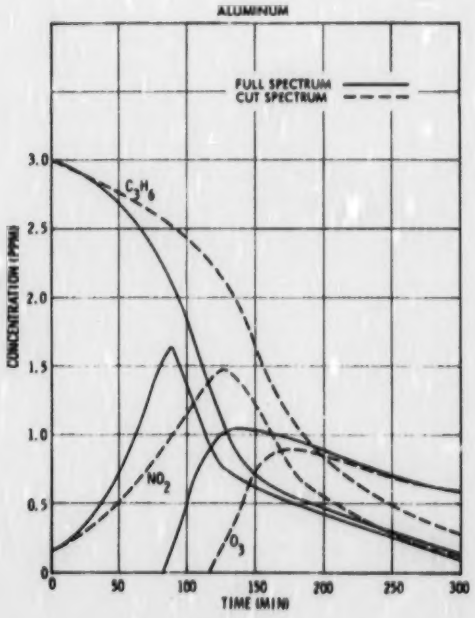

Fig. 3-3 Composite Photochemical Test Results for Aluminum Surfaces

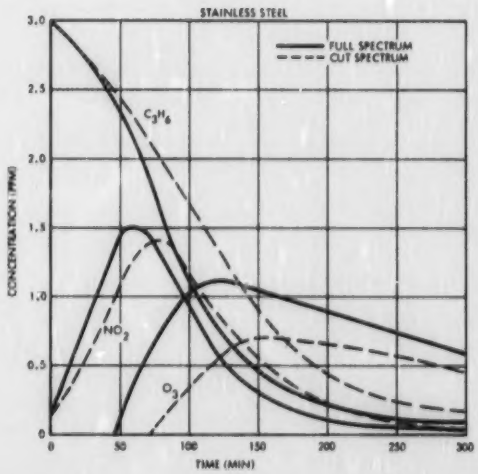

Fig. 3-4 Composite Photochemical Test Results for Stainless Steel Surfaces

Table 3-2

EFFECTS BY MATERIAL

(1) NO_2 FORMATION PARAMETERS

Effect	① NO_2 Rate				② NO_2 T_{max}				③ NO_2 Dose				⑱ NO_2 Dose Factor			
	Alum	Pyrex	Teflon	S.S.	Alum	Pyrex	Teflon	S.S.	Alum	Pyrex	Teflon	S.S.	Alum	Pyrex	Teflon	S.S.
m	13.1	10.0	8.63	25.4	106	131	154	70	176	178	219	153	39.0	39.2	48.7	34.5
A	0.35	-0.7	-0.26	13.5*	–	37.2*	-19.1*	-22.5*	14†	85*	-47*	- 4	2.5	16.7*	-10.5*	-0.7
B	4.42†	5.3†	2.77	9.3*	-38.5*	-74.2*	-67.5*	-28.0	-32*	-76*	-70*	-41*	-7.7*	-10.3*	-16.1*	-9.0*
C	-1.38	0.5	-1.71	-10.3*	8.0	- 3.2	16*	20.5*	10	-24*	- 2	14†	1.7	- 6.0*	- 1.8	4.2*
AB	-1.65	0.4	-0.09	3.1	6.0	-30.7	3	1.0	-10	-41	14	- 4	-2.5	-10.5	4.2	-1.2
AC	1.50	-1.5	-0.58	- 1.7	- 7.5	- 4.7	9	- 0.5	0.2	-29	11	4	-0.6	- 5.0	2.1	0.2
BC	-1.38	1.2	-0.06	- 0.6	4.0	- 6.2	7	- 8.0	- 5	21	15	- 6	-0.8	2.7	3.3	-2.7
ABC	0.10	-1.2	0.13	- 1.4	4.5	18.2	-12	1.0	1	33	- 7	- 1	0.5	6.0	- 1.5	-0.4
s		2.60				7.35				8.43				1.93		
10%		3.87				11.0				12.6				2.88		
1%		5.33				15.1				17.3				3.96		

Effect	⑳ NO_2 FWHM				㉑ Crossover Time				㉒ = ② - ㉑				⑰ NO Rate			
	Alum	Pyrex	Teflon	S.S.	Alum	Pyrex	Teflon	S.S.	Alum	Pyrex	Teflon	S.S.	Alum	Pyrex	Teflon	S.S.
m	99	103	125	86	56	78	82	38	50	58	70	36	8.71	8.55	7.20	14.4
A	6.2	27*	-19*	- 9†	- 1.7	12.5*	0.7	-14.0*	1.7	26.0*	-25.7*	- 8*	-0.08	- 2.06†	0.59	3.8*
B	-32.7*	-59*	-69*	-31*	-17.2*	-35.5*	-26.2*	-13.5*	-21.2*	-38.5*	-35.7*	-14*	2.60†	4.61*	2.45†	4.8*
C	1.2	- 9	9†	11	5.2	4.5	13.7	13.0*	2.2	- 7.5*	7.7*	8	-0.13	1.23	- 0.16	-1.9†
AB	0.7	-23	17	- 1	4.7	- 9.5	1.2	2.0	1.2	-20.5	6.7	- 1	-0.24	0.38	- 0.01	0.4
AC	- 5.2	-11	11	1	- 5.7	1.5	7.2	- 1.5	- 1.7	- 6.0	6.2	1	0.78	- 0.92	- 0.30	-0.3
BC	0.7	2	2	- 5	3.7	- 6.5	- 0.2	- 4.0	0.2	1.5	1.2	- 4	-0.23	1.56	- 0.06	0.7
ABC	2.2	15	- 3	- 1	2.7	6.5	- 4.2	1.5	1.7	13.5	-14.2	- 1	0.09	- 1.29	0.33	-0.2
s		4.83				4.18				2.91				1.29		
10%		7.20				6.23				4.33				1.92		
1%		9.90				8.57				5.97				2.69		

*Significant at 1% Level.
†Significant at 10% Level.

Table 3-2 (Cont.)

(2) OZONE PARAMETERS

Effect	④ Ozone Max Rate				⑤ Ozone Avg. Rate				⑥ Max Ozone Conc				⑦ Ozone T_{Max}			
	Alum	Pyrex	Teflon	S.S.	Alum	Pyrex	Teflon	S.S.	Alum	Pyrex	Teflon	S.S.	Alum	Pyrex	Teflon	S.S.
m	24.7	24.7	21.3	21.2	4.08	3.60	3.12	5.68	1.00	0.93	1.03	0.90	172	189	230	137
A	-9.7*	-8.5*	-1.4	-8.2*	- 0.66*	- 1.35*	0.20	- 0.01	- 0.14*	- 0.12*	-0.06	- 0.26	6	-58*	-31*	-18*
B	7.7*	8.2*	11.2*	10.8*	1.61*	2.18*	1.92*	3.35*	0.04	0.09*	0.20*	0.40*	-56*	-98*	-89*	-45*
C	0.9	4.5†	2.4	0.4	- 0.08	0.56*	0.16	- 1.05*	0.08*	0.13*	0.15*	0.05†	8	- 2	12†	25
AB	-3.7	4.4	-5.6	-1.9	- 0.21	0.01	- 0.11	- 0.01	0.02	- 0.01	-0.06†	- 0.03	2	-43	15	1.2
AC	-2.0	1.0	-1.2	-0.1	0.25	- 0.05	- 0.21	- 0.05	–	0.03	-0.04	- 0.02	- 9	-15	7	- 4
BC	-1.1	-0.4	-2.4	-0.5	- 0.13	0.39	- 0.20	0.02	–	0.01	-0.05	0.01	4	- 1	1	-10
ABC	0.9	-1.0	-0.5	1.1	–	- 0.56	0.08	0.01	–	- 0.03	–	0.02	3	27	8	4
s		2.66				0.258				0.033				8.05		
10%		3.97				0.385				0.049				12.0		
1%		5.45				0.529				0.068				16.5		

Effect	⑯ Max Pan Conc				㉓ = ⑦ - ㉑				⑧ Ozone Dose				⑲ Ozone Dose Factor			
	Alum	Pyrex	Teflon	S.S.	Alum	Pyrex	Teflon	S.S.	Alum	Pyrex	Teflon	S.S.	Alum	Pyrex	Teflon	S.S.
m	0.35	0.14	0.29	0.23	116	115	148	103	156	126	131	157	34.3	27.8	28.6	34.1
A	-0.05	0.04	-0.10*	-0.03	8.5†	46.0*	-30.5*	- 4	-22.0*	-48*	4.0	-29*	- 5.4*	-12.5*	1.9	- 6.4*
B	-0.11*	0.02	0.19*	0.01	-39.0*	-62.0*	-62.5*	-31*	38.0*	61*	94.5*	48*	7.9*	12.3*	20.6*	10.8*
C	0.03	-0.02	0.12*	0.02	2.5	- 6.5	- 1.0	11*	5.5	26*	9.5	- 4	0.9	4.2*	0.8	- 3.0†
AB	0.09	0.03	-0.12	0.07	- 3.0	-34.0	14.5	–	-11.0	15	21.0	-12	- 2.7	2.0	- 3.6	–
AC	-0.02	–	-0.06	0.01	- 3.5	-16.5	- 0.5	- 3	10.5	9	14.5	2	1.8	2.9	- 3.4	–
BC	0.04	0.03	0.03	0.03	1.0	5.5	0.5	- 6	- 8.5	3	11.5	8	- 1.7	- 0.7	- 2.5	0.8
ABC	-0.06	-0.01	-0.02	–	1.0	20.5	- 4.5	2	6.5	-13	8.0	3	1.5	- 3.1	1.7	0.6
s		0.039				4.86				8.51				1.68		
10%		0.058				7.24				12.7				2.50		
1%		0.080				9.96				17.4				3.44		

*Significant at 1% Level.
†Significant at 10% Level.

LOCKHEED MISSILES & SPACE COMPANY

Table 3-2 (Cont.)

(3) PROPYLENE PARAMETERS

Effect	⑨ HC Final Conc.				⑩ HC T 0.75				⑪ HC T 0.5				⑫ HC T 0.25			
	Alum	Pyrex	Teflon	S.S.	Alum	Pyrex	Teflon	S.S.	Alum	Pyrex	Teflon	S.S.	Alum	Pyrex	Teflon	S.S.
m	0.16	0.26	0.26	0.15	94	117	124	64	133	157	180	97	166	189	218	133
A	0.05	0.15*	-0.10*	-0.03	- 3	27*	–	-21*	3	44*	-15*	-22*	8	45*	-19*	-18*
B	-0.06†	- 0.19*	-0.24*	-0.09*	-28*	-56*	-38*	-20*	-43*	-76*	-70*	-34*	-48*	-80*	-84*	-45*
C	–	- 0.10*	-0.02	–	9	- 3	11	22*	12†	- 8	6	19*	7	-15*	4	19*
AB	-0.01	- 0.06	0.04	0.04	9	-18	- 4	4	7	-25	3	7	6	-26	6	4
AC	-0.01	- 0.10	0.04	-0.04	- 3	-11	–	-11	- 7	- 9	7	- 7	-10	-14	7	-11
BC	0.04	0.04	0.08	-0.02	9	4	- 1	- 9	7	- 1	4	- 9	7	5	7	-11
ABC	0.03	0.06	-0.08	0.02	- 8	18	–	7	- 2	22	- 8	3	2	26	- 9	5
s		0.039				8.34				6.85				6.76		
10%		0.058				12.4				10.2				10.1		
1%		0.080				17.1				14.0				13.9		

Effect	⑬ HC Max. Rate				⑭ HC Av. Rate				⑮ Max. Ald			
	Alum	Pyrex	Teflon	S.S.	Alum	Pyrex	Teflon	S.S.	Alum	Pyrex	Teflon	S.S.
m	21.8	23.6	15.9	23.9	11.5	10.1	8.2	16.2	0.87	0.70	0.75	0.76
A	-3.7†	-10.2*	4.0*	0.5	-0.85	- 2.2*	0.6	4.5*	- 0.13	- 0.40*	- 0.01	- 0.02
B	6.6*	13.5*	8.2*	9.2*	4.04*	- 5.3*	3.6*	5.8*	- 0.08	0.11	0.06	0.01
C	-0.8	0.9	2.2	1.4	-1.52	1.1	- 0.3	- 3.0*	- 0.10	–	- 0.02	- 0.06
AB	0.8	- 0.5	1.1	-0.4	-0.88	1.0	0.1	0.3	- 0.06	- 0.09	–	- 0.07
AC	2.9	0.8	-1.0	0.1	1.3	- 0.5	0.1	–	- 0.04	- 0.01	- 0.06	0.04
BC	1.2	- 0.2	0.3	1.3	-1.06	- 1.4	- 0.5	0.6	0.04	0.07	- 0.02	0.02
ABC	-0.8	2.0	0.6	-0.2	0.53	–	0.5	- 0.3	- 0.06	- 0.03	- 0.05	- 0.10
s			1.94				1.06				0.135	
10%			2.89				1.58				0.201	
1%			3.98				2.17				0.277	

*Significant at 1% Level.
†Significant at 10% Level.

LOCKHEED MISSILES & SPACE COMPANY

For example, consider the following data for NO_2 time-to-maximum for Teflon surfaces:

Run No.	A	B	C	Time
38	+	+	+	121
34, 35	+	+	-	103
42	-	+	+	142
43, 44	-	+	-	115
36, 39	+	-	+	192
37	+	-	-	162
40	-	-	+	193
41	-	-	-	205

Effect A is $[(121-142) + (103-115) + (192-193) + (162-205)]/4 = -19.1$
Effect B is $[(121-192) + (103-162) + (142-193) + (115-205)]/4 = -67.5$, etc.
Note the efficiency with which each data point is utilized. This is characteristic of full factorial experimental designs. Selected conditions were replicated, to provide data on reproducibility to determine whether effects are "real" or are due to random deviation in chamber behavior. In this preliminary analysis, these replicates are averaged to allow the orthogonal data treatment just described.

Deviations between replicates were used to obtain s, the estimated standard deviation of the parameter. For all four materials and 23 parameters, pooling of the deviations is justified. The significance levels are then calculated from the t value for the number of degrees of freedom and s. The "effects" found are compared to the 1-percent and 10-percent significance levels in data interpretation.

Practical considerations required that the experimental plan be conducted for each material and each S/V level as a subgroup. A time trend analysis (Appendix B) was thus conducted, to see if systematic drift was present in the experiment. Three sets of replicates are available, immediate reruns, reruns differing by more than 1 and less than 15 run numbers, and a complete rerun of the first material used in the experiment (run number differing by more than 50). Both the Rank Sum Test and the Sign Test show no compelling evidence of drift.

3.1 MATERIAL DIFFERENCES

The four materials may be grouped in terms of increasing NO_2 formation rate: Teflon, Pyrex, aluminum, stainless steel. Pyrex and aluminum are similar in behavior for most parameters. Other reactivity manifestations such as times to NO_2 maximum, ozone maximum, 50 percent propylene destruction, and NO_2 dose follow the same order. Preliminary correlation analyses indicate that stainless steel behaves in a different manner than do the other three materials.

3.2 EFFECT OF FACTORS

Of the three independent variables studied, the spectral change caused the largest change in behavior. For all four materials, the cutoff spectrum consistently and clearly slowed the reaction relative to the full spectrum. The following table shows the ratio of cut to full spectrum for several "reactivity" measures.

	Teflon	Pyrex	Aluminum	Stainless Steel
NO_2 T_{max} (1)	1.58	1.78	1.54	1.49
Ozone T_{max} (7)	1.49	1.68	1.47	1.39
50% Propylene Destruction (11)	1.50	1.64	1.47	1.43

Cleaning technique appreciably affected several of the behavior characteristics for the stainless steel system. S/V ratio measurably affected most parameters for the four materials.

Further analysis and interpretation of the data accumulated is underway, and will be reported upon in the Phase III final report. The behavior of acetaldehyde and PAN is being examined, and will be included in the Phase III work.

3.3 OZONE DECAY RESULTS

One parameter frequently used as a measure of chamber cleanliness is the ozone half-life in the smog chamber. Measurements were made of the ozone half-life in the chamber each time a new set of surface materials was installed, and when the S/V was changed. The conditions were: temperature, 95°F; relative humidity, 55°F dew-point; total HC as methane, < 0.1 ppm. The initial ozone concentration was 1 to 2 ppm. These tests were usually conducted in conjunction with the vacuum chamber off-gassing that was used as the final cleaning step after installing the new material. Ozone decay was determined in the dark and for the illuminator (full spectrum configuration) at its nominal 6,500-W power output (decay in the light). Results are shown in Table 3-3. Ozone decayed fastest in the presence of stainless steel surfaces and most slowly in the presence of Pyrex. It should be recognized that ozone decay behavior is a function of history as well as material and configuration, and, by itself, has been the subject of several research investigations (e.g., Sobersky et al., Environ. Sci. and Tech., Vol. 7, 1973, p. 347). Correlation of these results with the photochemical test results will be undertaken and reported in the Phase III report.

Table 3-3

OZONE HALF-LIFE STUDY

Configuration	Half-Life in Dark (min)	Half-Life in Light (min)
Base Chamber	430	180
Aluminum High S/V	270	210
Aluminum Low S/V	340	215
Pyrex High S/V	360	300
Pyrex Low S/V	340	275
Teflon High S/V	295	200
Teflon Low S/V	350	270
Stainless Steel High S/V	160	100
Stainless Steel Low S/V	190	120

Section 4
DISCUSSION

A number of reactions in the hydrocarbon-oxides of the nitrogen photochemical system are particularly sensitive to the low wavelength region of sunlight. These include:

1. a. $O_3 + h\nu \rightarrow O_2 (^1\Delta g) + O(^1D)$ (below 313 nm)
   b. $O(^1D) + H_2O \Delta 2HO^{\cdot}$
2. $H_2O_2 + h\nu \rightarrow 2HO^{\cdot}$ (below 340 nm)
3. $ROOH + h\nu \rightarrow RO^{\cdot} + HO^{\cdot}$ (below 300 nm)
4. $RCHO + h\nu \rightarrow R^{\cdot} + HCO^{\cdot}$ (below 352 nm)

The absorption cross sections for these substances is very low. However, reactions 1 through 3 lead to the very reactive hydroxyl radical, and reaction 4 also leads to reactive chain carriers.

The large effect of spectral distribution on photochemical reaction systems – at the same intensity as measured by k_d – has not previously been reported. However, some literature data are available that suggest that such an effect is not only present but may be general. Altshuler and Cohen (Ref. 5) reported a factor of 2 to 3 times higher NO_2 formation rates for tests in Teflon vs. Mylar containers. This difference was attributed to the difference in k_d of 0.35 to 0.4 min^{-1} for Teflon vs. 0.25 to 0.3 min^{-1} for the Mylar. The substantial difference in light below 330 nm for the two materials was noted, but not further discussed. This differential rate was observed for some 16 hydrocarbons, ranging in reactivity from 1, 3, 5 trimethylbenzene and 1, 2, 3, 5 tetramethylbenzene at the high reactivity end to ethylbenzene and toluene at the low reactivity end.

Table 4-1 gives a "Mylar/Teflon" spectral effect for time to NO_2 maximum calculated from Altshuler's data, after normalizing by the ratio of 0.275/0.325 to account for

the difference in k_d. Glasson and Tuesday (Ref. 6) give experimental data that show that NO_2 formation rate is linear with k_d for a variety of hydrocarbons. Such a linear factor is also suggested by Niki et al. (Ref. 7) as applicable to the early stages of the photochemical reaction. The difference in transmission characteristics for the Teflon vs. the Mylar containers results in a cut/full spectral distribution somewhat similar to that used in the present study. The spectral effect factor for propylene was 1.65.

A similar treatment of that data for oxygenates yields the following "Mylar/Teflon" spectral effect: formaldehyde 5.9, acetaldehyde 3.5, proprionaldehyde 3.9, acrolein 2.9, ethanol 1.6.

Table 4-1

"MYLAR/TEFLON" SPECTRAL EFFECT*

Hydrocarbon	Ratio of NO_2 T_{max}
Ethylene	2.93
Propylene	1.65
Isobutene	1.81
Toluene	1.76
Ethylbenzene	>2.7
1,2-dimethylbenzene	1.46
1,3-dimethylbenzene	1.32
1,4-dimethylbenzene	2.20
1,2-methylethylbenzene	1.74
1,3-methylethylbenzene	1.96
1,4-methylethylbenzene	2.29
1,3,5-trimethylbenzene	2.00
1,2-diethylbenzene	2.05
1,3-diethylbenzene	1.67
1,4-diethylbenzene	2.06
1,2,3,5-tetramethylbenzene	1.92

*Calculated from Ref. 5.

Bufalini et al. (Ref. 8) have reported that photooxidation of formaldehyde in the presence of NO_2 proceeded more rapidly at k_d of 0.14 min^{-1} with sunlamps than at 0.32 min^{-1} with blacklamps. This is an obvious result of the photodisintegration by the shorter wavelength light from the sunlamps. The time ratio for 50 percent consumption of formaldehyde, corrected for the k_d ratio, is 1.6 for the blacklamp/sunlamp distribution. For an irradiation without NO_2, the corrected time ratio for 37 percent consumption is 2.7.

The distribution of NO_2 photolysis events versus wavelength has been calculated for several spectral distributions. For this calculation, the wavelength interval between 290 and 410 nm is considered. Absorption coefficient (Ref. 9) and quantum yield (Ref. 10) for NO_2 are tabulated at 10-nm intervals in this interval. These multiplied by each other and by the number of photons in the 10-nm wavelength interval gives the total NO_2 photolysis rate. This total rate divided into the events in each 10-nm band gives the fractional distribution of NO_2 photolysis events, or shows how the same k_d occurs for different spectra. Figure 4-1 gives the results.

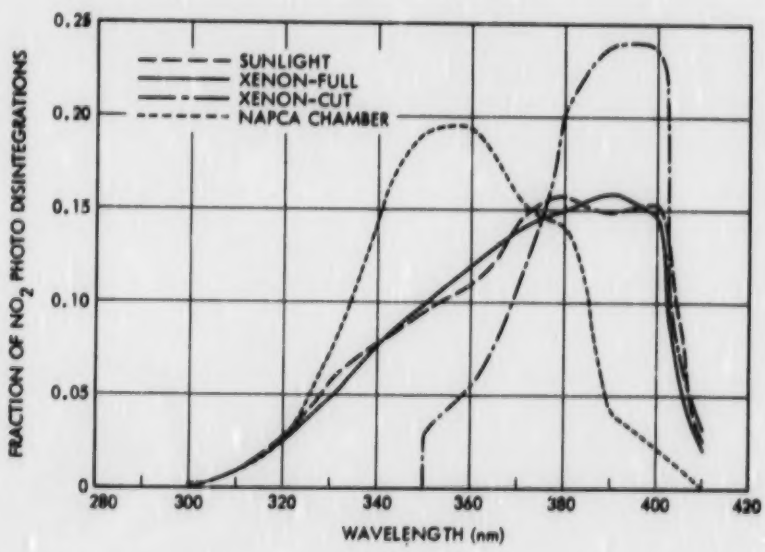

Fig. 4-1 Distribution of NO_2 Photodisintegrations for Various Spectra

The sunlight curve is for high noon in Los Angeles or Stanford, Conn. (two distributions averaged) (Refs. 11,12); the xenon-full and xenon-cut are for the spectra used in this study, as previously shown in Fig. 2-6. The NAPCA chamber curve is for the spectral distribution given by Korth et al. (Ref. 13), which is one of the few reported chamber spectra in the literature.

The xenon-full NO_2 disintegration spectral distribution does indeed closely match the sunlight curve, over the entire wavelength interval. The NAPCA chamber distribution is probably typical of chambers illuminated by fluorescent tube combinations, and shows that the wavelength band from 335 to 365 nm is overemphasized (relative to the sunlight distribution), while the 385–410 nm band is underrepresented. This disparity is frequently unrecognized in discussing the application of smog chamber data to atmospheric simulation.

It is clear that the spectral distribution of light provided a smog chamber influences the photochemical reaction observed. In particular, the NO_2 photodisintegration rate (k_d or its equivalent k_1) dies not sufficiently characterize the light conditions.

Section 5
FUTURE WORK

5.1 ONGOING WORK

Further work on this project is being conducted. Photochemical runs for the butane/NO_x system are underway. The question of relative humidity effects is under study, by a series of runs at low relative humidity (5 to 10 percent) to yield comparison data with the runs discussed, which were at 25 percent relative humidity.

Further analysis of the completed experimental program also is underway. A covariance analysis is being conducted, to refine the linear extrapolation method used to account for varying initial NO_2 content in the NO_x. A multivariate analysis will also be conducted, to group run parameters and allow better estimation of effects.

This effort will then be utilized to synthesize a model that may be used to account for differences reported in the behavior of various environmental chambers.

5.2 RECOMMENDED FURTHER WORK

Following completion of the scheduled ongoing work discussed above, further investigations are recommended.

a. Conduct a similar set of tests for another hydrocarbon/NO_x system, such as m-xylene/NO_x. This will indicate whether the observed spectral effects are general, as the range of organic species from unreactive aliphatic (butane), reactive olefin (propylene), and reactive aromatic (m-xylene) will then be available. Also use of a range of compounds from unreactive gas to polar high-boiling liquid may show differing cleaning effects.

b. Perform further studies of the spectral effect, by varying the cutoff wavelength. By use of Teflon rather than Pyrex chamber faces, the amount of light at wavelengths below 320 nm can be substantially increased. Evidently this lower wavelength light is disproportionately important in smog photochemistry. A second new spectrum to investigate is one that has a cutoff between the 320 and 350 nm spectra just investigated. Having available spectral effect data for four cutoffs, it is then possible to obtain an important function for the wavelength range.

c. Determine the spectral distribution for the various smog chambers compared by the Project group, and in conjunction with the importance function generated in item b above, normalize chamber data. Spectral distribution determination could be done on a calculational or experimental basis.

d. Investigate light intensity effects by a set of tests at 50 percent and 150 percent of the light intensity previously used. It is fairly well established that initial behavior of the photochemical system is linear with light intensity, but how late smog manifestations, such as ozone maximum concentration and PAN build-up, vary is not well known. Such data will also be helpful in applying chamber data to the atmospheric diurnal intensity variation.

e. Searching for explanations of persistent anomalies in smog chamber behavior would be productive. Among such anomalies not well understood at present are the occurrence of peak NO_2 concentrations greater than initial NO_x charged (for fast reacting systems such as propylene); the initial induction period in NO disappearance; and the entire nitrogen balance. One technique for such an investigation would be to utilize an alternative detection method for the nitrogen species to correlate with the Saltzman NO_2 and the chemiluminescent NO. Fourier Transform Spectroscopy is such a technique, and arrangements may be made for such a spectrometer.

REFERENCES

1. Coordinating Research Council, Individual Hydrocarbon Reactivity Measurements: State-of-the-Art, CRC Report No. 398, New York, Jun 1966
2. D. B. Wimmer, "Factors Affecting Reactions in Environmental Chambers," Coordinating Research Council Inc., Air Pollution Research Advisory Committee Symposium, Chicago, May 1971
3. R. J. Jaffe, Factors Affecting Reactions in Environmental Chambers, Phase I, LMSC-A997745, 20 May 1972
4. O. L. Davies (ed.), The Design and Analysis of Industrial Experiments, Ch. 7, "Factorial Experiments," p. 247, Hafner Publishing Co., New York 1956
5. A. P. Altshuler and I. R. Cohen, "Structural Effects on the Rate of Nitrogen Dioxide Formulation in the Photooxidation of Organic Compound-Nitric Oxide Mixtures in Air," Int. J. Air Wat. Poll., Vol. 7, 1963, p. 787
6. W. A. Glasson and C. S. Tuesday, "Hydrocarbon Reactivity and the Kinetics of the Atmospheric Photooxidation of Nitric Oxide," J. Air Pollution Control Assoc., Vol. 20, 1970, p. 239
7. H. Niki, E. E. Daby, and B. Weinstock, "Mechanisms of Smog Reactions," Advan. Chem., Vol. 13, 1972, p. 16
8. J. J. Bufalini, B. W. Gay, and K. L. Brubaker, "Hydrogen Peroxide Formation From Formaldehyde Photo Oxidation and Its Presence in Urban Atmospheres," Env. Sci. Tech., Vol. 6, 1972, p. 816
9. P. A. Leighton, Photochemistry of Air Pollution, Academic Press, 1961
10. R. J. Gordon, in National Air Pollution Control Administration Pub. 999-AP-38
11. R. C. Hirt et al., Ultraviolet Spectral Energy Distributions of Natural Sunlight and Accelerated Test Light Sources, J. Opt. Soc. Am., Vol. 50, 1960, p. 706
12. J. S. Nader, in National Air Pollution Control Administration Pub. 999-AP-38
13. M. W. Korth, A. H. Rose, and R. C. Stahman, "Effects of Hydrocarbon to Oxides of Nitrogen Ratios on Irradiated Auto Exhaust," Part I, J. Air Pollution Control Assoc., Vol. 14, 1964, p. 168

Appendix A
PHOTOCHEMICAL RUN DATA

Photochemical run data are given in this appendix in two forms – a plot of NO, NO_2, ozone, and propylene vs irradiation time, and the tabulation of the calculated run parameters as defined in Table 3-1. Data at 10 or 15 minute intervals are available for acetaldehyde and PAN, but only the maximum for these species is reported in the tables. The materials order is aluminum, Pyrex, Teflon, and stainless steel. Eight run graphs are shown for each material. These are for the eight combinations of S/V, spectrum, and cleaning investigated, and are arranged in sequence as follows:

S/V	Spectrum	Cleaning
High	Full	Vac
High	Full	Purge
Low	Full	Vac
Low	Full	Purge
High	Cut	Vac
High	Cut	Purge
Low	Cut	Vac
Low	Cut	Purge

For each material and variable combination, the average of the replicates of the individual runs is given. Each run was separately analyzed, to obtain the 23 parameters given in the tabulation.

Initial condition variations affect some of the run parameters rather strongly. For this preliminary analysis of the data, the only initial condition accounted for is the initial percentage of NO_2 in the NO_x. As previously suggested, both on theoretical and experimental grounds (Niki, Ref. 7, and B. Dimitriades, Bureau of Mines RI 7433), this is accounted for by a linear extrapolation along the time axis to the standard reference

starting condition of 10 percent NO_2 content in NO_x. The tabulated run data show this adjustment as the column T ADJ. For the runs used in the effects analysis, the largest value of T ADJ is 12 minutes. The covariance and multivariate analyses will further refine initial condition adjustments, and will be discussed in the Phase III report.

It will be noted that two complete sets of experiments were performed for aluminum surfaces. Changes were made in the instrumentation after runs 3 through 6 in the test sequence. These changes made the set of runs between run 69 and run 85 better suited for the effects analysis. In addition, as experience in operating the smog chamber accumulated, better control of initial conditions was obtained. The difference in means between the early and late aluminum tests is given in Table B-3 (page B-8). The average percent difference is 7.6 (excluding parameter 15). The effects as calculated for the early and late sets of aluminum runs are similar. The data accumulated in the late set of aluminum runs is preferable for the reasons just mentioned, and are the ones reported.

This page is intentionally blank.

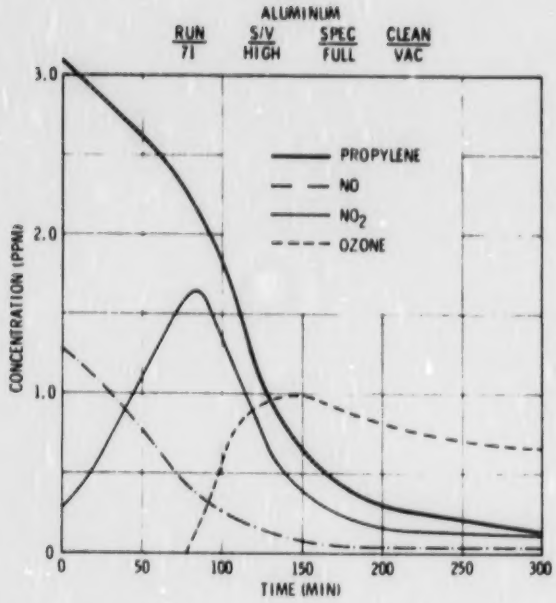

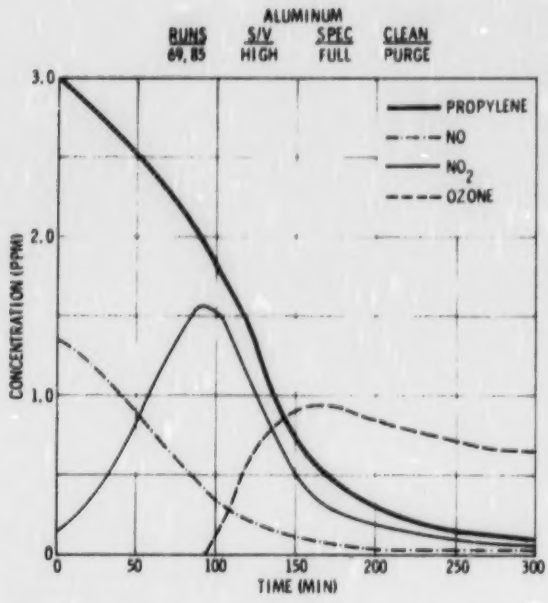

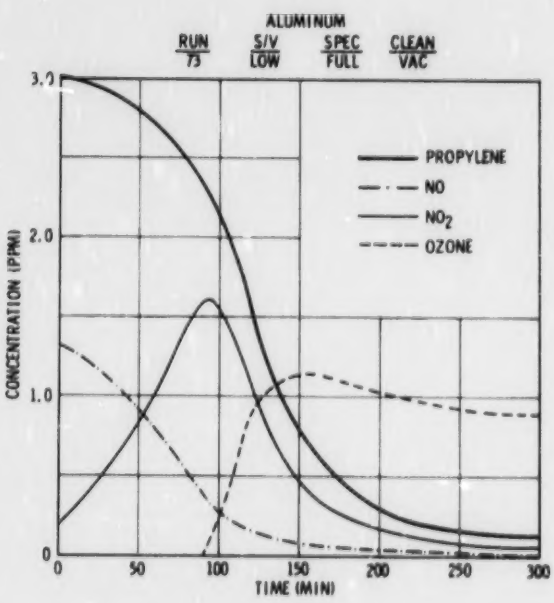

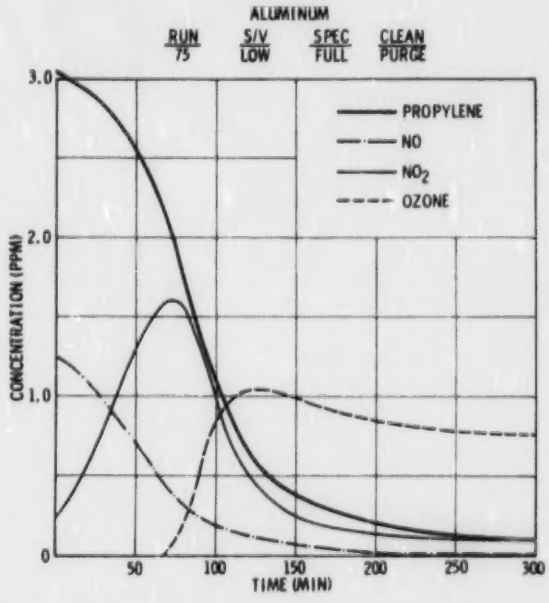

Preceding page blank

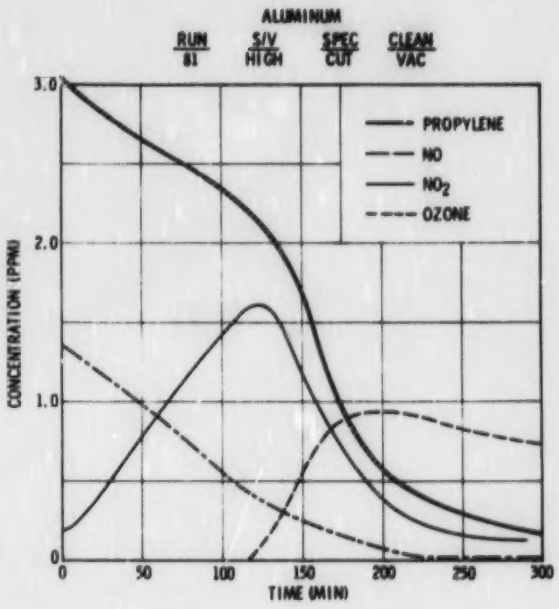
ALUMINUM
RUN 81
S/V HIGH
SPEC CUT
CLEAN VAC
PROPYLENE
NO
NO2
OZONE
CONCENTRATION (PPM)
TIME (MIN)
0
1.0
2.0
3.0
0
50
100
150
200
250
300

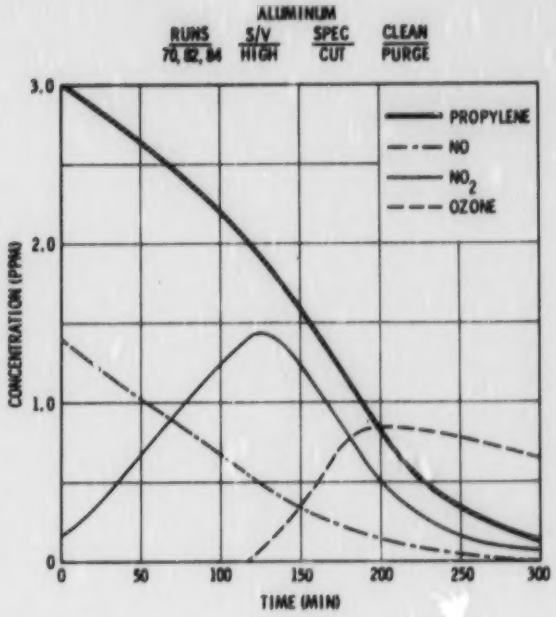
ALUMINUM
RUNS 70, 82, 84
S/V HIGH
SPEC CUT
CLEAN PURGE
PROPYLENE
NO
NO2
OZONE
CONCENTRATION (PPM)
TIME (MIN)
0
1.0
2.0
3.0
0
50
100
150
200
250
300

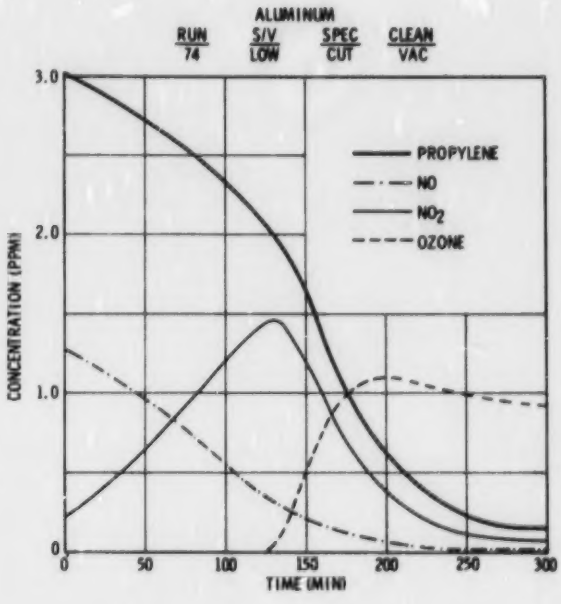
ALUMINUM
RUN 74
S/V LOW
SPEC CUT
CLEAN VAC
PROPYLENE
NO
NO2
OZONE
CONCENTRATION (PPM)
TIME (MIN)
0
1.0
2.0
3.0
0
50
100
150
200
250
300

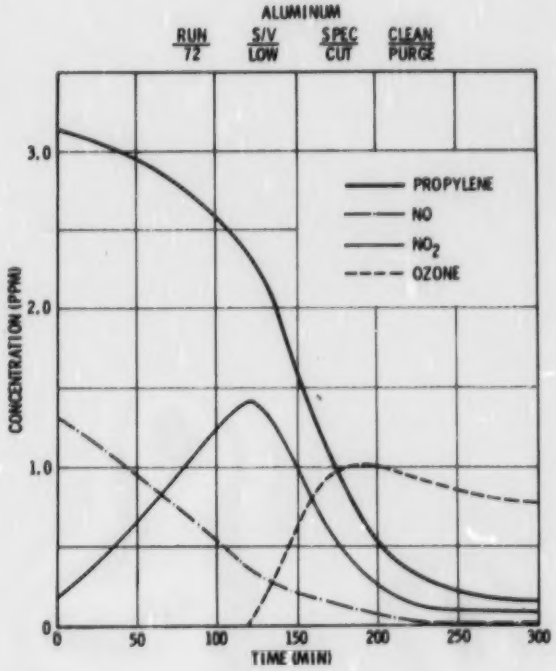
ALUMINUM
RUN 72
S/V LOW
SPEC CUT
CLEAN PURGE
PROPYLENE
NO
NO2
OZONE
CONCENTRATION (PPM)
TIME (MIN)
0
1.0
2.0
3.0
0
50
100
150
200
250
300

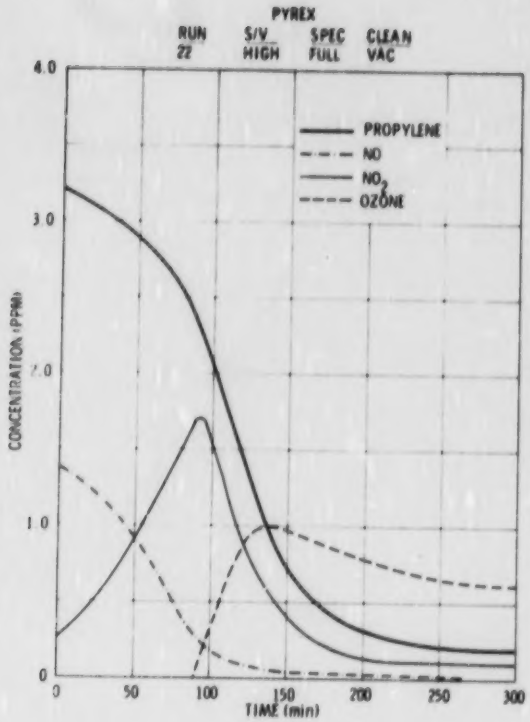
PYREX
RUN 22
S/V HIGH
SPEC FULL
CLEAN VAC
PROPYLENE
NO
NO2
OZONE
CONCENTRATION (PPM)
TIME (min)

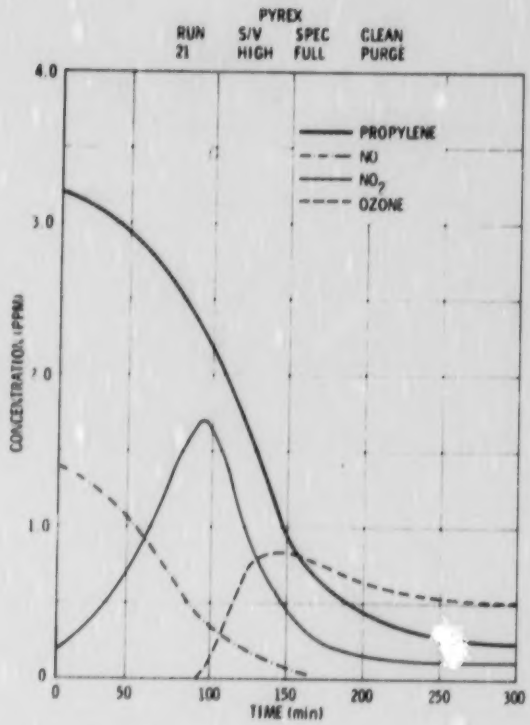
PYREX
RUN 21
S/V HIGH
SPEC FULL
CLEAN PURGE
PROPYLENE
NO
NO2
OZONE
CONCENTRATION (PPM)
TIME (min)

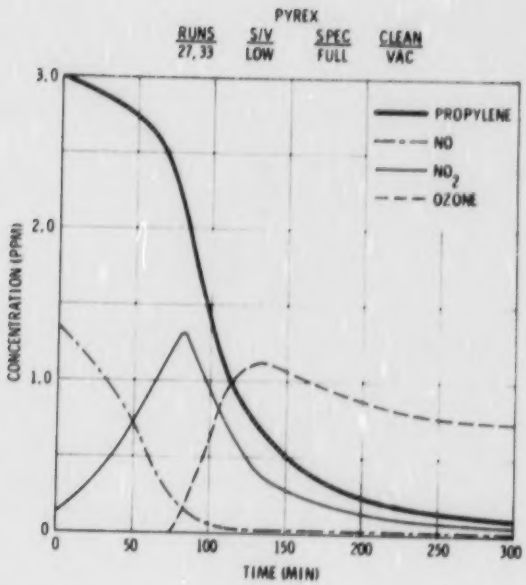
PYREX
RUNS 27, 33
S/V LOW
SPEC FULL
CLEAN VAC
PROPYLENE
NO
NO2
OZONE
CONCENTRATION (PPM)
TIME (MIN)

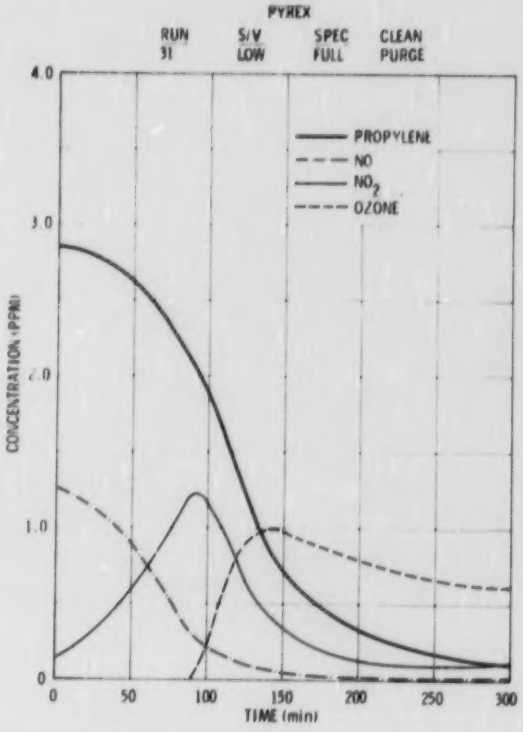
PYREX
RUN 31
S/V LOW
SPEC FULL
CLEAN PURGE
PROPYLENE
NO
NO2
OZONE
CONCENTRATION (PPM)
TIME (min)

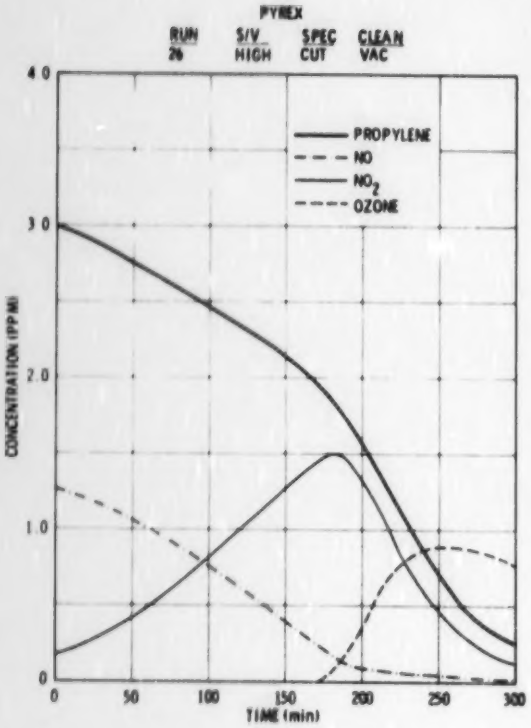
PYREX
RUN 26 S/V HIGH SPEC CUT CLEAN VAC
PROPYLENE
NO
NO2
OZONE
CONCENTRATION (PPM)
TIME (min)

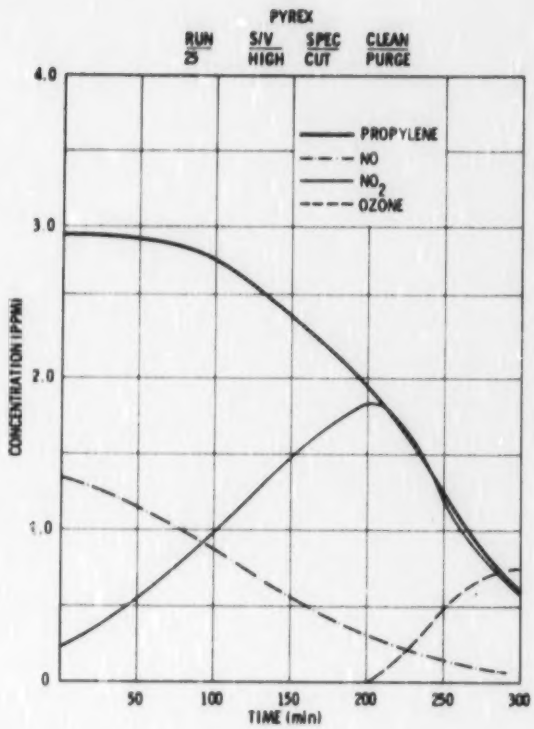
PYREX
RUN 25 S/V HIGH SPEC CUT CLEAN PURGE
PROPYLENE
NO
NO2
OZONE
CONCENTRATION (PPM)
TIME (min)

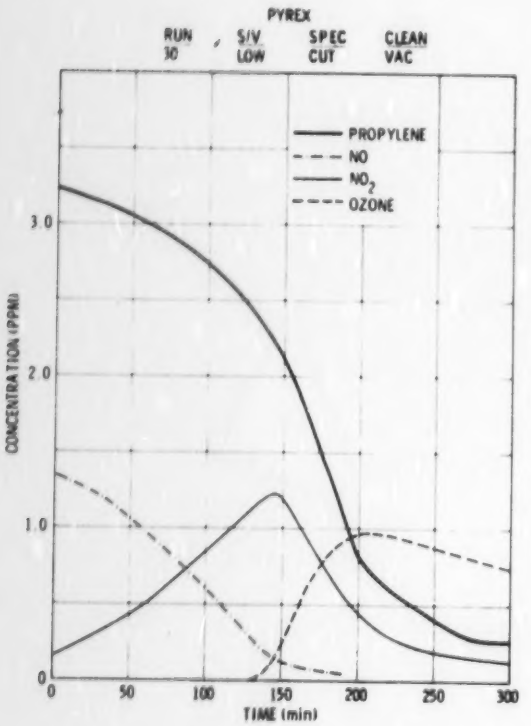
PYREX
RUN 30 S/V LOW SPEC CUT CLEAN VAC
PROPYLENE
NO
NO2
OZONE
CONCENTRATION (PPM)
TIME (min)

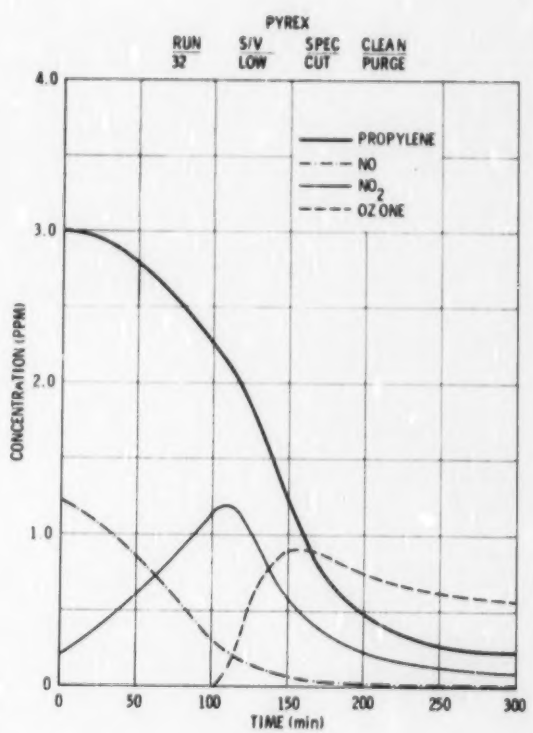
PYREX
RUN 32 S/V LOW SPEC CUT CLEAN PURGE
PROPYLENE
NO
NO2
OZONE
CONCENTRATION (PPM)
TIME (min)

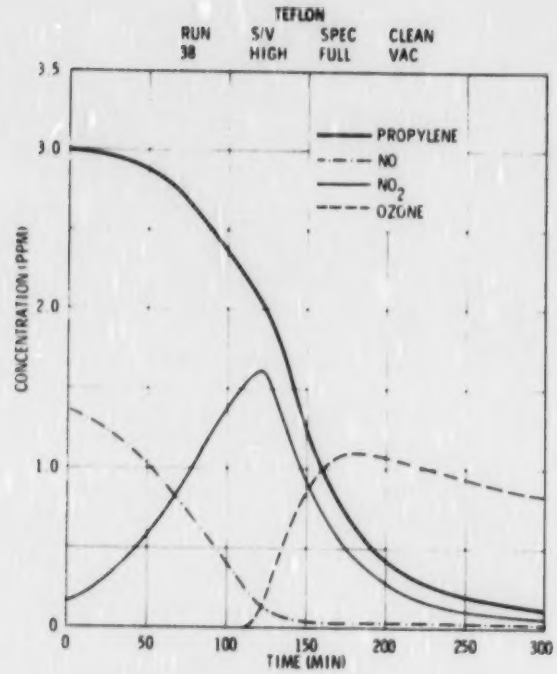
TEFLON
RUN 38
S/V HIGH
SPEC FULL
CLEAN VAC
PROPYLENE
NO
NO2
OZONE
CONCENTRATION (PPM)
TIME (MIN)

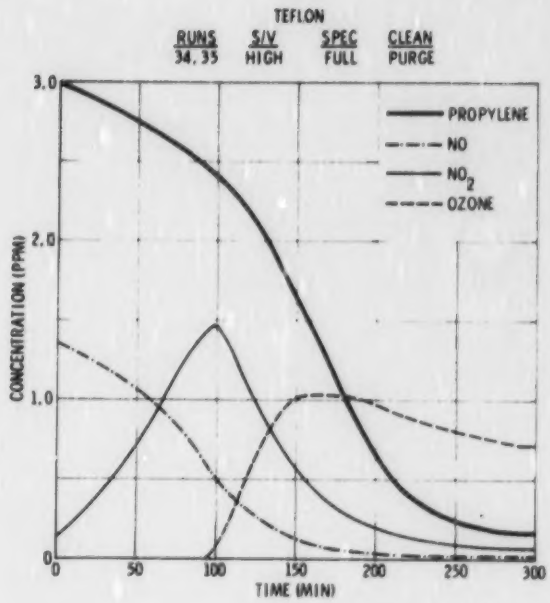
TEFLON
RUNS 34, 35
S/V HIGH
SPEC FULL
CLEAN PURGE
PROPYLENE
NO
NO2
OZONE
CONCENTRATION (PPM)
TIME (MIN)

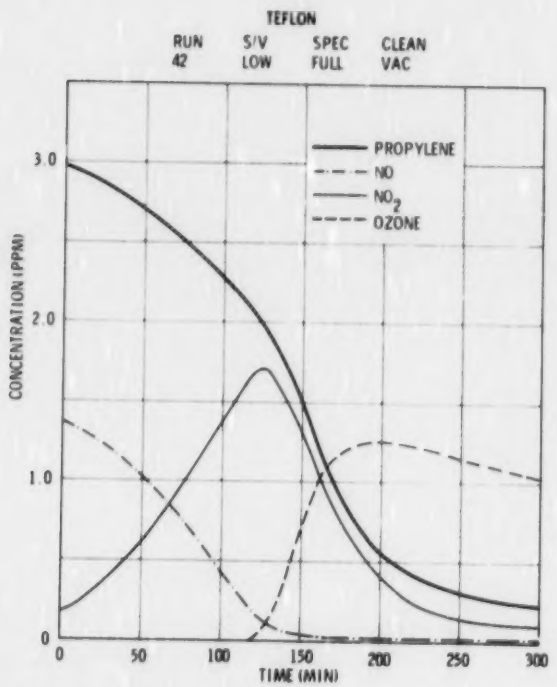
TEFLON
RUN 42
S/V LOW
SPEC FULL
CLEAN VAC
PROPYLENE
NO
NO2
OZONE
CONCENTRATION (PPM)
TIME (MIN)

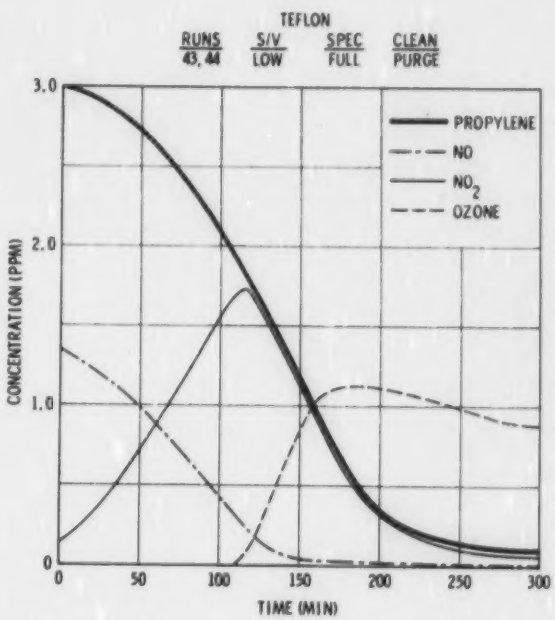
TEFLON
RUNS 43, 44
S/V LOW
SPEC FULL
CLEAN PURGE
PROPYLENE
NO
NO2
OZONE
CONCENTRATION (PPM)
TIME (MIN)

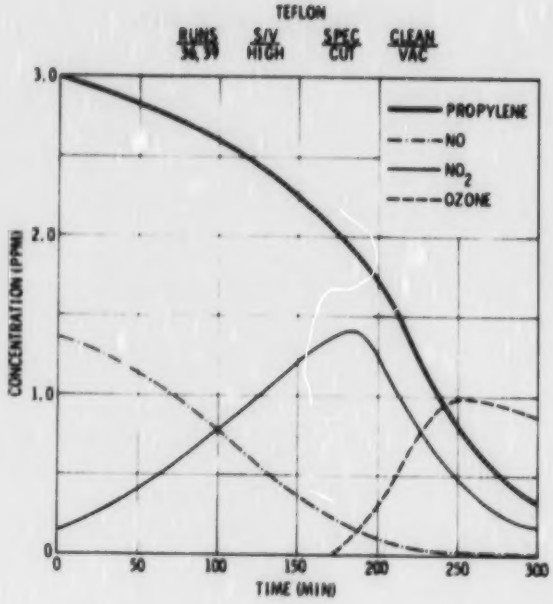
TEFLON
RUNS 36, 39
S/V HIGH
SPEC CUT
CLEAN VAC
PROPYLENE
NO
NO2
OZONE
CONCENTRATION (PPM)
TIME (MIN)

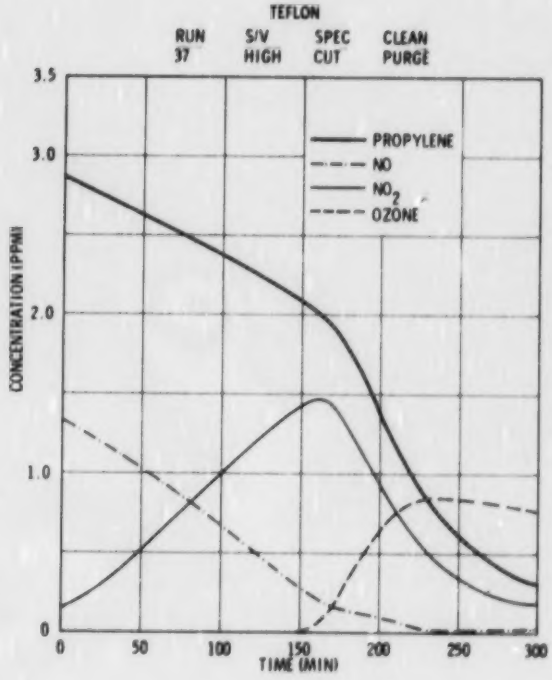
TEFLON
RUN 37
S/V HIGH
SPEC CUT
CLEAN PURGE
PROPYLENE
NO
NO2
OZONE
CONCENTRATION (PPM)
TIME (MIN)

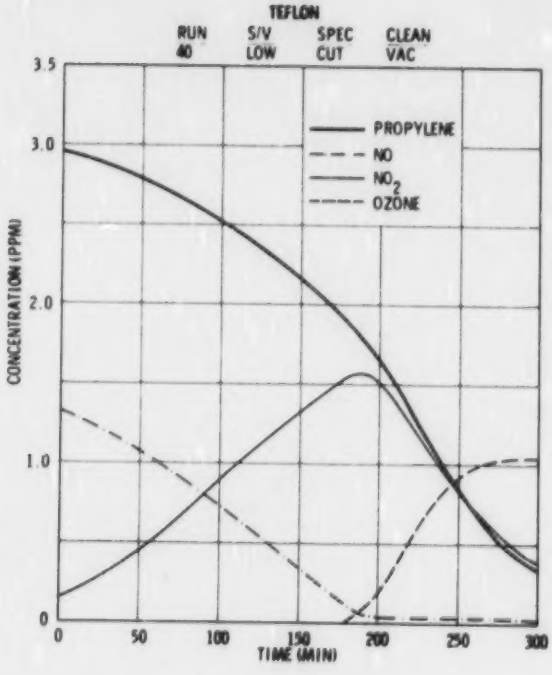
TEFLON
RUN 40
S/V LOW
SPEC CUT
CLEAN VAC
PROPYLENE
NO
NO2
OZONE
CONCENTRATION (PPM)
TIME (MIN)

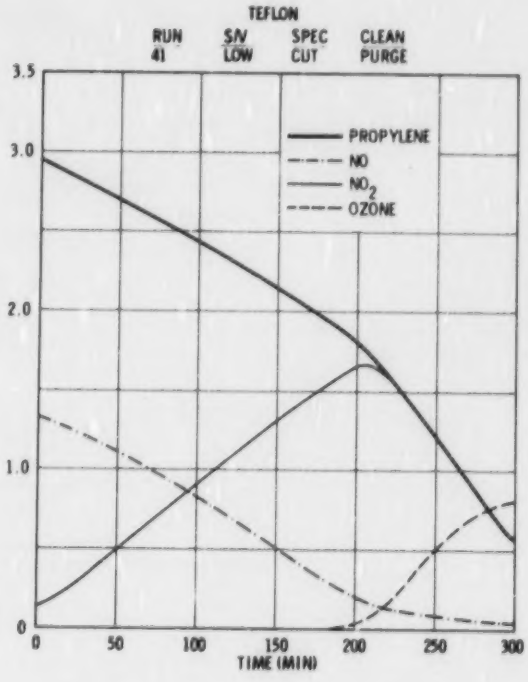
TEFLON
RUN 41
S/V LOW
SPEC CUT
CLEAN PURGE
PROPYLENE
NO
NO2
OZONE
CONCENTRATION (PPM)
TIME (MIN)

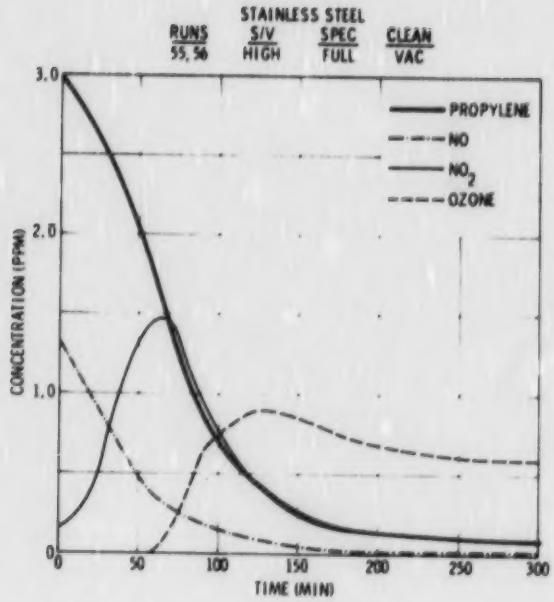
STAINLESS STEEL
RUNS 55, 56
S/V HIGH
SPEC FULL
CLEAN VAC
PROPYLENE
NO
NO2
OZONE
CONCENTRATION (PPM)
TIME (MIN)
0
1.0
2.0
3.0
50
100
150
200
250
300

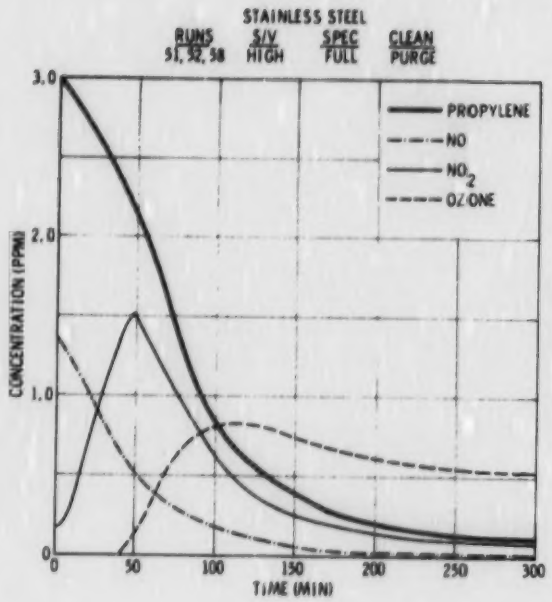
STAINLESS STEEL
RUNS 51, 52, 58
S/V HIGH
SPEC FULL
CLEAN PURGE
PROPYLENE
NO
NO2
OZONE
CONCENTRATION (PPM)
TIME (MIN)
0
1.0
2.0
3.0
50
100
150
200
250
300

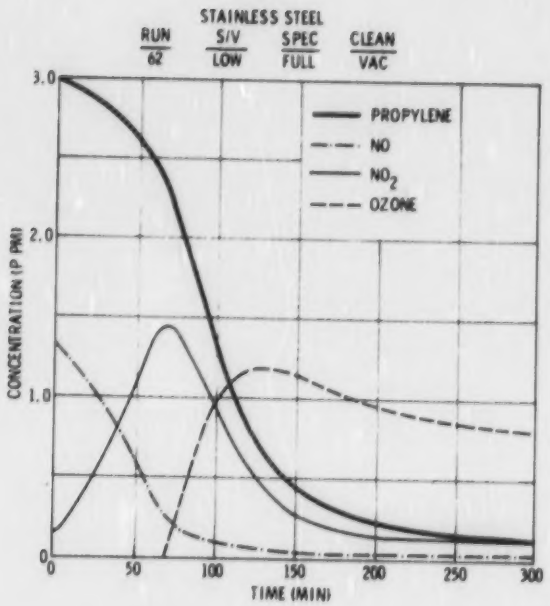
STAINLESS STEEL
RUN 62
S/V LOW
SPEC FULL
CLEAN VAC
PROPYLENE
NO
NO2
OZONE
CONCENTRATION (PPM)
TIME (MIN)
0
1.0
2.0
3.0
50
100
150
200
250
300

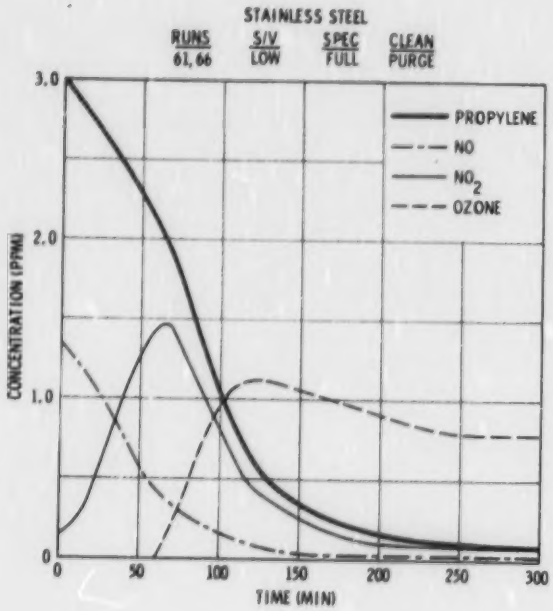
STAINLESS STEEL
RUNS 61, 66
S/V LOW
SPEC FULL
CLEAN PURGE
PROPYLENE
NO
NO2
OZONE
CONCENTRATION (PPM)
TIME (MIN)
0
1.0
2.0
3.0
50
100
150
200
250
300

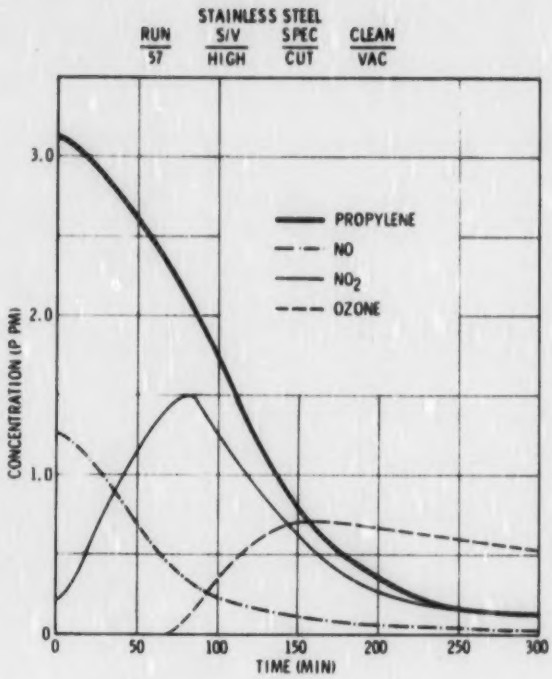
STAINLESS STEEL
RUN 57
S/V HIGH
SPEC CUT
CLEAN VAC
PROPYLENE
NO
NO2
OZONE
CONCENTRATION (P PM)
TIME (MIN)

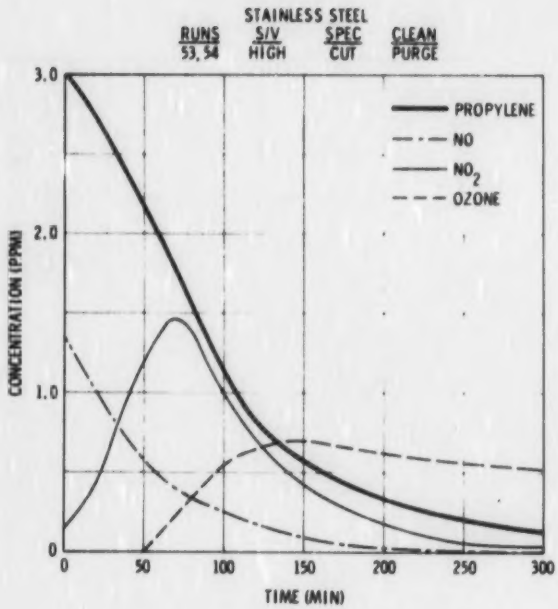
STAINLESS STEEL
RUNS 53, 54
S/V HIGH
SPEC CUT
CLEAN PURGE
PROPYLENE
NO
NO2
OZONE
CONCENTRATION (PPM)
TIME (MIN)

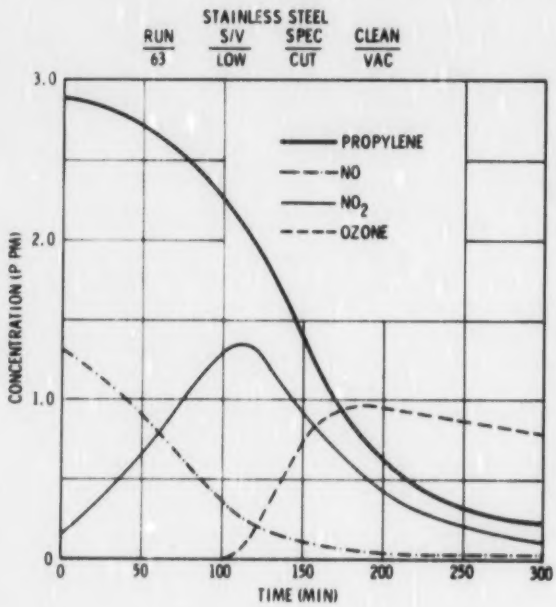
STAINLESS STEEL
RUN 63
S/V LOW
SPEC CUT
CLEAN VAC
PROPYLENE
NO
NO2
OZONE
CONCENTRATION (P PM)
TIME (MIN)

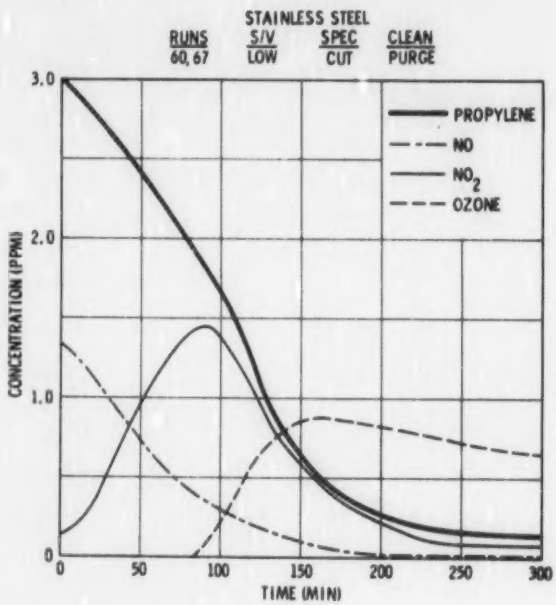
STAINLESS STEEL
RUNS 60, 67
S/V LOW
SPEC CUT
CLEAN PURGE
PROPYLENE
NO
NO2
OZONE
CONCENTRATION (PPM)
TIME (MIN)

TITLE- ALUM

	RUNNO	STOV	SPEC	CLEAN	HCINIT	NOX	NO2	PCNO2	TADJ	HCNOX	① NO2R
1#	3.0	1	1	1	3.17	1.52	.22	14.5	9	2.09	15.10
2#	71.0	1	1	1	3.10	1.52	.25	16.4	12	2.00	14.00
3#	4.0	1	1	-1	3.05	1.54	.29	18.8	17	1.98	15.80
4#	4.5	1	1	-1	2.90	1.41	.29	20.6	21	2.06	13.00
5#	69.0	1	1	-1	3.04	1.47	.21	14.3	8	2.07	14.70
6#	85.0	1	1	-1	2.94	1.49	.13	8.7	-2	1.97	16.00
7#	10.0	-1	1	1	2.96	1.51	.31	20.5	20	1.96	15.80
8#	11.0	-1	1	1	3.03	1.43	.22	15.4	11	2.12	13.20
9#	73.0	-1	1	1	3.00	1.47	.14	9.5	0	2.02	13.80
10#	12.0	-1	1	-1	2.98	1.51	.11	7.3	-8	1.97	13.10
11#	12.5	-1	1	-1	2.83	1.67	.36	19.2	18	1.69	15.50
12#	75.0	-1	1	-1	3.06	1.45	.19	13.1	6	2.11	18.10
13#	6.0	1	-1	1	2.81	1.59	.31	19.5	28	2.04	10.10
14#	81.0	1	-1	1	3.04	1.49	.14	9.4	-2	2.04	12.60
15#	5.0	1	-1	-1	2.98	1.33	.12	9.0	0	2.24	8.40
16#	70.0	1	-1	-1	2.88	1.47	.17	11.6	4	1.96	8.78
17#	82.0	1	-1	-1	3.07	1.49	.17	11.4	4	2.06	13.70
18#	84.0	1	-1	-1	2.96	1.41	.14	8.5	0	2.10	11.10
19#	9.0	-1	-1	1	2.94	1.49	.33	22.1	35	1.97	7.79
20#	74.0	-1	-1	1	3.02	1.46	.16	12.3	6	2.07	9.23
21#	7.0	-1	-1	-1	2.84	1.42	.22	15.5	16	2.00	9.28
22#	8.0	-1	-1	-1	2.92	1.36	.19	14.0	12	2.15	8.03
23#	72.0	-1	-1	-1	3.00	1.46	.15	10.3	0	2.15	10.60

TITLE- ALUM

	RUN2NO	② NO2TM	③ NO2DOS	④ O3MAXR	⑤ O3AVGR	⑥ O3MAXC	⑦ O3TM	⑧ O3DOSE	⑨ HCFC	⑩ HCT75
1#	3.0	79	142	22.8	4.46	.82	129	135	.05	70
2#	71.0	94	165	21.3	4.55	1.00	152	165	.18	86
3#	4.0	77	142	32.5	5.84	1.04	122	165	.10	69
4#	4.5	81	128	30.9	5.53	1.05	121	158	.10	64
5#	69.0	83	152	21.9	4.48	.94	143	144	.14	76
6#	85.0	88	166	22.1	4.23	.93	148	158	.10	82
7#	10.0	81	145	30.3	6.09	1.15	140	200	.19	81
8#	11.0	86	146	37.3	5.54	1.12	131	190	.15	83
9#	73.0	91	160	35.6	5.18	1.13	149	181	.12	91
10#	12.0	92	159	31.7	5.38	1.14	137	189	.13	85
11#	12.5	92	168	28.9	5.31	1.04	138	193	.14	91
12#	75.0	76	157	34.7	5.47	1.04	131	201	.10	63
13#	6.0	125	178	19.2	3.24	.92	190	133	.15	101
14#	81.0	118	211	17.4	3.29	.94	198	140	.18	104
15#	5.0	107	123	17.6	2.72	.77	165	114	.35	96
16#	70.0	144	200	18.0	2.71	.90	219	112	.31	107
17#	82.0	114	206	22.1	3.02	.84	189	133	.22	103
18#	84.0	120	186	13.8	2.73	.83	210	121	.27	88
19#	9.0	145	176	23.0	2.74	.92	205	116	.31	148
20#	74.0	136	188	26.2	3.48	1.10	206	147	.16	111
21#	7.0	124	159	22.8	3.32	.91	176	127	.27	128
22#	8.0	125	140	26.7	3.38	.96	177	135	.28	132
23#	72.0	120	172	21.2	3.52	1.02	190	137	.17	116

TITLE- ALUM	(11)	(12)	(13)	(14)	(15)	(16)	(17)	(18)	(19)
RUN3NO	HCT50	HCT25	HCMAXR	HCAVGR	ALDMAX	PANMAX	NORATE	NO2DF	O3DF
1# 3.0	100	127	27.4	15.80	.60	.56	12.50	31.1	28.5
2# 71.0	122	152	24.9	12.30	.70	.31	10.10	35.5	35.5
3# 4.0	99	131	25.1	15.40	.55	1.10	14.20	31.6	36.7
4# 4.5	105	132	23.1	14.70	.51	1.10	12.20	30.3	37.3
5# 69.0	108	143	22.0	13.60	.72	.38	10.50	33.6	31.8
6# 85.0	118	149	22.9	12.50	.83	.29	8.70	35.9	34.2
7# 10.0	109	141	24.8	13.20	.59	.13	12.80	32.1	44.2
8# 11.0	111	143	27.2	13.30	.60	.17	11.10	34.0	44.3
9# 73.0	120	146	25.7	12.20	1.00	.35	9.56	35.5	40.2
10# 12.0	119	142	27.0	12.80	.50	.30	11.00	35.1	41.7
11# 12.5	118	145	26.3	11.50	.54	.33	11.80	33.5	38.5
12# 75.0	92	124	27.4	16.60	.86	.20	10.80	34.7	44.4
13# 6.0	148	184	18.3	10.30	.77	.23	9.93	37.3	27.9
14# 81.0	153	185	17.0	9.67	.86	.35	7.88	46.0	30.5
15# 5.0	137	190	17.8	10.70	.73	.32	9.03	30.9	28.5
16# 70.0	165	211	13.2	8.10	.94	.37	6.70	45.6	25.6
17# 82.0	144	186	18.2	10.10	.92	.33	7.70	45.2	29.2
18# 84.0	147	194	14.8	9.89	.82	.26	6.90	43.1	28.0
19# 9.0	180	210	23.6	7.54	.49	.18	7.36	39.4	26.0
20# 74.0	161	195	17.9	8.87	.90	.45	7.04	42.1	32.9
21# 7.0	159	204	21.0	8.37	.52	.16	8.77	37.3	29.8
22# 8.0	160	203	21.6	8.63	.58	.14	7.82	34.3	33.1
23# 72.0	151	182	23.7	10.10	.98	.50	7.62	38.5	30.6

TITLE- ALUM	(20)	(21)	(22)	(23)
RUN4NO	FWHM	XTIME	NO2XT	O3XT
1# 3.0	73	43	36	86
2# 71.0	86	52	42	100
3# 4.0	66	44	33	78
4# 4.5	70	47	34	74
5# 69.0	89	44	39	99
6# 85.0	85	49	39	99
7# 10.0	74	43	38	97
8# 11.0	67	49	37	82
9# 73.0	82	52	39	97
10# 12.0	72	52	40	85
11# 12.5	73	48	44	90
12# 75.0	77	40	36	91
13# 6.0	110	66	59	124
14# 81.0	115	58	60	140
15# 5.0	89	64	43	101
16# 70.0	126	76	68	143
17# 82.0	110	56	58	138
18# 84.0	131	63	57	147
19# 9.0	117	82	63	123
20# 74.0	117	73	63	133
21# 7.0	101	64	60	112
22# 8.0	97	71	54	106
23# 72.0	109	63	57	127

TITLE- PYREX ①

RUN1NO	STOV	SPEC	CLEAN	HCINIT	NOX	NO2	PCNO2	TADJ	HCINOX	NO2R
1# 22	1	1	1	3.22	1.68	.27	16.1	12	1.92	12.80
2# 21	1	1	-1	3.20	1.57	.17	10.8	0	2.04	13.50
3# 27	-1	1	1	2.94	1.55	.18	11.6	5	1.90	13.50
4# 33	-1	1	1	3.00	1.52	.16	10.5	0	1.97	15.00
5# 31	-1	1	-1	2.84	1.39	.14	10.1	0	2.04	10.10
6# 26	1	-1	1	2.98	1.44	.18	12.5	7	2.07	6.25
7# 25	1	-1	-1	2.95	1.54	.21	13.6	10	1.92	7.26
8# 30	-1	-1	1	3.23	1.50	.16	10.7	2	2.15	7.58
9# 32	-1	-1	-1	3.00	1.43	.20	14.0	11	2.10	8.10

TITLE- PYREX ② ③ ④ ⑤ ⑥ ⑦ ⑧ ⑨ ⑩

RUN2NO	NO2TM	NO2DOS	O3MAXR	O3AVGR	O3MAXC	O3TMAX	O3DOSE	HCFC	HCT75
1# 22	99	163	28.8	4.19	.98	152	152.9	.16	98
2# 21	95	161	24.7	3.85	.84	143	127.5	.26	89
3# 27	78	116	36.3	6.56	1.16	122	187.7	.08	70
4# 33	79	114	32.9	6.13	1.11	125	190.0	.11	81
5# 31	102	122	28.8	4.58	.98	140	156.0	.13	87
6# 26	192	225	17.7	2.17	.92	267	80.7	.30	149
7# 25	212	332	10.6	1.49	.73	310	41.5	.64	185
8# 30	147	161	28.5	3.02	.97	207	127.8	.26	133
9# 32	121	144	25.6	3.36	.91	166	126.5	.24	111

TITLE- PYREX ⑪ ⑫ ⑬ ⑭ ⑮ ⑯ ⑰ ⑱ ⑲

RUN3NO	HCT50	HCT25	HCMAXR	HCAVGR	ALDMAX	PANMAX	NORATE	NO2DF	O3DF
1# 22	130	159	26.8	12.00	.70	.15	10.30	32.0	30.3
2# 21	125	157	23.3	12.30	.68	.15	9.72	34.2	27.1
3# 27	88	117	34.0	16.40	.96	.11	12.70	24.8	43.4
4# 33	98	128	34.6	15.10	.88	.16	14.20	24.8	41.1
5# 31	120	150	36.8	11.70	.77	.13	9.19	29.1	37.4
6# 26	210	235	12.0	6.67	.64	.14	5.07	52.1	19.9
7# 25	249	295	12.1	5.20	.68	.18	5.00	72.0	9.0
8# 30	172	203	22.9	8.92	.57	.12	7.10	35.9	28.4
9# 32	148	183	20.6	9.52	.65	.12	7.81	33.6	29.5

TITLE- PYREX ⑳ ㉑ ㉒ ㉓

RUN4NO	FWHM	XTIME	NO2XT	O3XT
1# 22	74	61	42	91
2# 21	77	55	40	88
3# 27	63	50	28	72
4# 33	66	50	29	75
5# 31	77	60	42	80
6# 26	138	106	86	161
7# 25	176	100	114	210
8# 30	115	89	59	118
9# 32	100	73	48	93

TITLE- TEFLON

RUNINO	STOV	SPEC	CLEAN	HCINIT	NOX	NO2	PCNO2	TADJ	HCINOX	NO2R (1)
1# 38	1	1	1	3.00	1.52	.16	10.5	0	1.97	8.72
2# 34	1	1	-1	2.82	1.38	.13	9.4	-2	2.04	11.30
3# 35	1	1	-1	2.86	1.50	.15	14.7	14	1.91	11.10
4# 42	-1	1	1	2.97	1.54	.18	11.7	5	1.93	9.52
5# 43	-1	1	-1	2.98	1.52	.15	14.5	13	1.96	11.60
6# 44	-1	1	-1	3.03	1.47	.15	13.6	10	2.06	10.50
7# 36	1	-1	1	2.99	1.63	.17	10.4	0	1.84	6.19
8# 39	1	-1	1	2.96	1.45	.17	11.7	7	2.04	5.91
9# 37	1	-1	-1	2.86	1.48	.15	10.1	0	1.93	8.11
10# 40	-1	-1	1	2.98	1.49	.17	11.4	5	1.99	6.87
11# 41	-1	-1	-1	2.96	1.47	.14	9.5	-2	2.01	7.56

TITLE- TEFLON

RUN2NO	NO2TM (2)	NO2DOS (3)	O3MAXR (4)	O3AVGR (5)	O3MAXC (6)	O3TMAX (7)	O3DOSE (8)	HCFC (9)	HCT75 (10)
1# 38	121	176	22.5	4.04	1.10	183	166.0	.12	109
2# 34	102	151	23.6	4.33	1.04	168	166.0	.09	95
3# 35	104	167	24.8	4.09	1.04	174	181.0	.12	102
4# 42	142	205	31.3	4.08	1.25	200	189.0	.22	112
5# 43	116	203	32.9	4.08	1.12	176	189.0	.08	105
6# 44	113	188	26.2	3.90	1.10	195	180.0	.15	98
7# 36	180	217	20.2	2.42	1.01	260	94.8	.32	136
8# 39	203	228	19.6	2.25	.98	267	97.0	.32	166
9# 37	162	223	15.7	2.28	.85	237	97.9	.30	139
10# 40	193	267	16.4	2.33	1.05	295	93.0	.34	147
11# 41	205	303	10.8	1.67	.80	298	50.0	.56	136

TITLE- TEFLON

RUN3NO	HCT50 (11)	HCT25 (12)	HCMAXR (13)	HCAVGR (14)	ALDMAX (15)	PANMAX (16)	NORATE (17)	NO2DF (18)	O3DF (19)
1# 38	143	174	23.6	10.20	.70	.31	8.61	38.6	36.4
2# 34	133	161	21.3	10.50	.74	.25	8.86	36.4	40.0
3# 35	134	169	21.7	10.30	.95	.23	8.77	36.5	39.5
4# 42	156	190	18.8	9.05	.82	.61	7.99	44.3	39.8
5# 43	143	175	13.4	10.30	.79	.39	8.67	44.3	39.6
6# 44	144	177	18.7	10.20	.73	.34	7.86	42.4	39.8
7# 36	205	246	12.7	6.81	.70	.25	6.24	44.4	19.4
8# 39	224	262	14.0	6.11	.72	.21	5.33	52.9	21.0
9# 37	197	241	13.1	6.70	.72	.18	6.65	50.1	22.0
10# 40	217	263	12.0	6.39	.73	.25	5.92	59.8	19.8
11# 41	230	282	8.5	5.80	.72	.12	5.41	68.6	11.3

TITLE2 TEFLON

RUN4NO	FWHM (20)	XTIME (21)	NO2XT (22)	O3XT (23)
1# 38	90	78	43	105
2# 34	86	58	42	110
3# 35	91	63	41	111
4# 42	84	73	70	127
5# 43	93	63	53	122
6# 44	102	60	53	122
7# 36	143	107	85	157
8# 39	142	107	85	157
9# 37	140	82	58	155
10# 40	165	96	97	199
11# 41	190	94	111	204

TITLE- SSTEEL

	RUN1NO	STOV	SPEC	CLEAN	HCINIT	NOX	NO2	PCNO2	TADJ	HCNOX	① NO2R
1#	55	1	1	1	3.19	1.48	.15	10.1	0	2.16	33.5
2#	56	1	1	1	3.04	1.52	.18	11.8	0	2.00	29.1
3#	51	1	1	-1	3.09	1.42	.15	10.6	0	2.18	49.2
4#	52	1	1	-1	3.11	1.43	.15	10.5	0	2.17	45.7
5#	58	1	1	-1	2.86	1.49	.17	11.4	0	1.92	41.3
6#	62	-1	1	1	3.02	1.46	.15	10.3	0	2.07	17.8
7#	61	-1	1	-1	2.98	1.50	.16	10.7	0	1.99	26.8
8#	66	-1	1	-1	3.06	1.48	.16	10.8	0	2.07	24.4
9#	57	1	-1	1	3.11	1.44	.17	11.8	0	2.16	21.0
10#	53	1	-1	-1	3.05	1.49	.16	10.7	0	2.05	35.3
11#	54	1	-1	-1	3.24	1.52	.17	11.2	2	2.13	26.4
12#	63	-1	-1	1	2.88	1.44	.13	9.0	0	2.00	10.8
13#	60	-1	-1	-1	3.02	1.55	.18	11.6	3	1.95	21.2
14#	67	-1	-1	-1	3.00	1.53	.18	11.8	3	1.96	19.2

TITLE- SSTEEL

	② RUN2NO	NO2TM	③ NO2DOS	④ O3MAXR	⑤ O3AVGR	⑥ O3MAXC	⑦ O3TMAX	⑧ O3DOSE	⑨ HCFC	⑩ HCT75
1#	55	51	133	23.2	6.77	.88	115	162	.10	51
2#	56	53	134	20.9	6.87	.91	110	169	.11	49
3#	51	38	121	22.2	8.16	.81	90	159	.10	44
4#	52	37	116	21.6	8.04	.82	95	146	.15	39
5#	58	43	133	19.5	7.50	.85	110	164	.14	44
6#	62	73	139	31.1	6.86	1.18	130	200	.10	71
7#	61	58	135	32.9	8.00	1.12	110	194	.08	50
8#	66	63	134	31.7	7.70	1.15	120	210	.12	58
9#	57	86	186	12.5	3.43	.69	163	118	.14	71
10#	53	53	157	12.6	4.72	.68	135	130	.17	48
11#	54	65	164	13.3	4.40	.71	137	133	.20	64
12#	63	111	181	20.0	3.50	.96	190	136	.27	111
13#	60	81	174	16.5	4.34	.85	153	147	.11	61
14#	67	80	158	19.6	4.50	.89	143	147	.27	64

TITLE- SSTEEL

	⑪ RUN3NO	HCT50	⑫ HCT25	⑬ HCMAXR	⑭ HCAVGR	⑮ ALDMAX	⑯ PANMAX	⑰ NORATE	⑱ NO2DF	⑲ O3DF
1#	55	73	103	33.0	21.5	.60	.23	17.90	30.0	36.4
2#	56	77	107	26.7	19.3	.74	.27	18.10	29.4	32.0
3#	51	71	104	26.3	22.1	.55	.23	18.80	28.3	37.4
4#	52	64	100	26.9	23.5	.85	.25	20.00	27.1	39.1
5#	58	71	104	28.3	19.7	.91	.26	19.40	29.8	36.8
6#	62	94	124	29.8	15.7	.82	.21	14.30	31.8	45.7
7#	61	79	110	25.4	18.8	.79	.18	16.80	30.0	43.0
8#	66	82	113	28.8	18.2	.82	.26	15.00	30.2	47.3
9#	57	112	155	19.9	13.7	.81	.20	12.30	43.0	27.4
10#	53	86	132	18.5	17.6	.79	.16	16.00	35.0	29.1
11#	54	97	146	20.5	16.3	.71	.13	14.20	35.9	29.1
12#	63	148	190	18.7	9.2	.61	.29	9.03	41.9	31.6
13#	60	111	146	19.3	13.3	.79	.23	12.00	37.3	31.7
14#	67	113	148	18.5	12.9	.89	.28	11.00	33.7	31.5

TITLE- SSTEEL (20) (21) (22) (23)

RUN4NO	FWHM XTIME	NO2XT	O3XT
1# 55	70 25	26	90
2# 56	67 26	27	84
3# 51	60 17	21	78
4# 52	61 17	20	78
5# 58	64 18	25	92
6# 62	78 38	35	92
7# 61	75 27	31	83
8# 66	69 31	32	89
9# 57	107 40	46	123
10# 53	88 23	30	112
11# 54	89 29	36	108
12# 63	113 59	52	131
13# 60	100 38	43	115
14# 67	97 40	40	103

Appendix B
STATISTICAL ANALYSIS

The hypothesis to be tested concerns the presence of a steady drift over time regardless of the variables of material, surface to volume ratio, spectrum, or cleaning. If such a drift were present, then runs which are duplicates with respect to these four variables might be expected to differ by an amount which grows steadily as a function of the separation over time. Our attention is then focused upon an examination of the differences as a function of the time separation.

Note that the time separations of duplicates tend to fall into three basic groups:

1. Nine sequence numbers differing by one ($\Delta_t = 1$), i.e., immediate reruns:

4 – 4A (AL)	34 – 35 (T)
7 – 8 (AL)	43 – 44 (T)
10 – 11 (AL)	51 – 52 (SS)
12 – 12A (AL)	53 – 54 (SS)
	55 – 56 (SS)

Note: AL = aluminum; P = Pyrex; T = Teflon; SS = stainless steel

2. Ten sequence numbers differing by more than 1 but less than 20:

27 – 33 (P)	$\Delta_t = 6$	61 – 66 (SS)	$\Delta_t = 5$
36 – 39 (T)	$\Delta_t = 3$	70 – 82 (AL)	$\Delta_t = 12$
51 – 58 (SS)	$\Delta_t = 7$	70 – 84 (AL)	$\Delta_t = 14$
52 – 58 (SS)	$\Delta_t = 6$	69 – 85 (AL)	$\Delta_t = 16$
60 – 67 (SS)	$\Delta_t = 7$	82 – 84 (AL)	$\Delta_t = 2$

3. Long term replicates – a complete rerun of the aluminum experiment ($\Delta_t^s > 50$).

In the analysis, we concentrate on the differences between duplicate pairs, since this provides a direct basis for comparison. In the absence of drift, these pairs should be distributed around a central value of zero. If there is drift, then the pairs separated further apart in time (or sequence) could be expected to center about a value, different from zero and increasing in absolute magnitude as the separation increases. Note, however, that the long term replicates (group 3) all involve only one material, aluminum, and that each set of runs (initial aluminum, replicate aluminum) was fairly compact in time. In this case, one might anticipate a different kind of drift from what might occur during a single series. Thus, we distinguish two types of drift – drifts within a compact series of runs on a given material and drifts from material to material, or series to series.

The drifts within materials can be studied using the shorter term replicates, groups 1 and 2, while the drifts across materials or series can be studied by comparing the mean values across materials, especially between the initial aluminum set and the final replicate aluminum set.

B.1 DRIFTS WITHIN MATERIALS

If there is a drift within material, then the replicates with longer separations, group 2, should be centered around a different value than those of group 1. Hence we test the hypothesis that both sets are centered about the same central value. The test used is the rank sum test using the value of T' defined as follows. Arrange two samples (of differences) in order of size, and assign rank scores to the individual observations; score 1 for the smallest, 2 for the second smallest, etc. Then T' is the sum of the ranks of the observations in the smaller of the two sets. Using the Dixon and Massey tables*, we reject the hypothesis if the calculated score is significantly large or significantly small. From those tables we find that for a sample with $N_1^{**} = 8$ and $N_2^{*} = 7$,

*W. J. Dixon and F. J. Massey, Introduction to Statistical Analysis, McGraw Hill, New York, 1957.

**One complication in application is the triple formed by runs 51, 52 and 58, and 70, 82 and 84. Clearly we are not justified in forming three pairs. We have avoided this by dropping the middle run from consideration, thus leaving in the replicate difference involving the largest time separation, (51 minus 58) and (70 minus 84). The end result is 8 short-term replicates in group 1 and 7 longer term replicates in group 2.

the significant values are $T'_{\alpha} = 41$ and $T'_{1-\alpha} = 71$ for $\alpha = 0.047$. Thus, values of $T' \leq 41$ and ≥ 71 form a 9.4 percent critical region for the hypothesis.

The rank scores, calculated in the manner described for each of the 20 parameters, are shown in Table B-2. From the table, it can be seen that only parameter 13 qualifies as significant.

Here, we are confronted with a matter of judgment; by selecting a slightly more stringent criterion for significance, we would have found no significant scores. Using what is believed to be a conservative significance level, only one parameter – and that parameter not one that had previously stood out as particularly suspect of indicating a trend – is in the significant zone. All in all, the conclusion must be that we do not have compelling evidence of drift in this case.

Next, we turn our attention to a second hypothesis suggested by the data. Is the central value of all differences significantly different from zero? For this we use the sign test; that is, the number of positive and the number of negative differences are counted (when the difference is zero, this is excluded and the sample size reduced). Letting r represent the lesser of the two counts, and N the sample size, we obtain Table B-2. The null hypothesis of no difference from zero is rejected if r is too small. In particular (from Dixon and Massey, Table A-10a*), a value of r of 2 or less is significant at the 5 percent (two-tailed) level, for N = 12, 13, or 14 and 3 for N = 15. Thus, from Table B-2, parameters 11, 12, and 14 are significant. Parameters 1, 2, 5, 9, and 13 are close. Of these 8 parameters, we can determine whether or not the long term comparison on aluminum indicates a trend in the same direction. This leads to the following:

		Apparent Direction of Long Term Trend	
		Up	Down
Apparent Direction of Short Term Trend	Up	1	5, 14
	Down	2, 11	9, 12, 13

*W. J. Dixon and F. J. Massey, Introduction to Statistical Analysis, McGraw Hill, New York, 1957

Table B-1

DIFFERENCES OF REPLICATES

Parameter		1	2	3	4	5	6	7	8	9	10	11	12
4-4A	1	2.8	- 4	13	1.6	0.31	-0.01	1	7	0	5	- 6	- 1
7-8	1	1.25	- 1	19	-3.9	-0.06	-0.05	- 1	8	-0.01	- 4	- 1	1
10-11	1	2.6	- 5	- 1	-7.0	0.55	0.03	9	0	0.04	- 2	- 2	- 2
12-12A	1	-2.4	0	- 9	2.8	0.07	0.10	- 1	- 4	-0.01	- 6	1	- 3
34-35	1	.2	- 2	-16	-1.2	0.24	0	- 6	-15	-0.03	- 7	- 1	- 8
43-44	1	1.10	3	15	6.7	0.18	0.02	-19	9	-0.07	7	- 1	- 2
51-52*	1*	3.5*	1*	5*	0.6*	0.09*	-0.01*	- 5*	13*	-0.05*	5*	7*	- 4*
53-54	1	8.9	-12	-13	-0.7	0.32	-0.03	- 2	- 3	-0.03	-16	-11	- 6
55-56	1	4.4	- 2	- 1	2.3	-0.10	-0.03	5	- 7	-0.01	2	- 4	- 4
82-84*	2*	2.6*	- 6*	20*	8.3*	0.29*	0.01*	-21*	12*	-0.05*	15*	- 3*	- 8*
36-39	3	0.28	-23	-11	0.6	0.17	0.03	- 7	- 2.2	0	-30	-19	-16
61-66	5	2.40	- 5	1	1.2	0.30	-0.03	-10	-16	-0.04	- 8	- 3	- 3
27-33	6	-3.0	- 2	4	5.9	0.86	0.10	- 6	25	-0.05	-22	-19	-21
52-58*	6*	4.4*	- 6*	-17*	2.1*	0.54*	-0.03*	-15*	-18*	0.01*	- 5*	- 7*	- 4*
51-58	7	7.9	- 5	-12	2.7	0.66	-0.04	-20	- 5	-0.04	0	0	0
60-67	7	2.0	1	16	-3.1	-0.36	-0.04	10	0	-0.16	- 3	- 2	- 2
70-82*	12*	-4.92*	30*	- 6*	-2.1*	-0.31*	0.06*	30*	-21*	0.09*	4*	21*	25*
70-84	14	-2.32	24	14	4.2	-0.02	0.07	9	- 9	0.04	19	18	17
69-85	16	-1.30	- 5	- 6	-0.2	0.25	0.01	- 5	-14	0.04	- 6	-10	- 6
$\hat{S}$ (17df)		2.60	7.35	8.43	2.66	0.258	0.033	8.05	8.51	0.039	8.34	6.85	6.76

*Not used in rank sum or sign test.

Table B-1 (Cont.)

Parameter		13	14	15	16	17	18	19	20	21	22	23
4-4A	1	2.0	0.70	0.04	0	5.6	1.3	-0.6	- 4	- 3	- 1	4
7-8	1	-0.6	-0.26	-0.06	0.02	0.95	3.0	-3.3	4	- 2	6	6
10-11	1	-2.4	-0.01	-0.01	-0.04	-0.40	-1.9	-0.1	7	- 6	- 6	15
12-12A	1	0.7	1.30	-0.04	-0.03	-0.80	1.6	3.2	- 1	4	- 4	- 5
34-35	1	-0.4	0.20	-0.21	0.02	0.09	-0.1	0.5	- 5	- 5	1	- 1
43-44	1	-0.53	0.10	0.06	0.05	0.81	1.9	-0.2	- 9	3	0	0
51-52*	1*	-0.6*	-1.40*	-0.30*	-0.02*	-1.20*	1.2*	3.3*	- 1*	0	1*	0*
53-54	1	-2.0	1.30	0.08	0.03	1.80	-0.9	0	- 1	- 6	- 6	- 4
55-56	1	6.3	2.20	-0.14	-0.04	-0.20	0.6	-0.6	3	- 1	- 1	6
82-84*	2*	3.4*	0.21*	0.10*	0.07*	0.80*	2.1*	1.2*	-21*	- 7	1*	- 9*
36-39	3	-1.3	0.70	-0.02	0.04	0.93	-8.5	-1.6	1	0	0	0
61-66	5	-3.4	0.60	-0.03	-0.03	1.80	-0.2	-4.3	6	- 4	- 1	- 6
27-33	6	-1.1	2.70	0.16	-0.10	-2.90	0.5	4.6	- 6	1	- 3	- 7
52-58*	6*	-1.4*	3.80*	-0.06*	-0.01*	0.60*	-2.7*	-2.7*	- 3*	- 1*	- 5*	-14*
51-58	7	-2.0	2.40	0.66	-0.03	-0.60	-1.6	0.6	- 4	- 1	- 4	- 4
60-67	7	0.8	0.40	-0.36	-0.10	1.0	3.6	0.2	3	- 1	3	12
70-82*	12*	-5.0*	-2.00*	0.02*	0.04*	-1.0*	0.4*	-3.6*	16*	20*	10*	5*
70-84	14	-1.6	-1.79	0.12	0.11	-0.2	2.5	-2.4	- 5	13	11	- 4
69-85	16	-0.9	1.10	-0.11	0.09	1.8	-2.3	-2.4	4	- 5	0	0
$\hat{S}$ (17df)		1.94	1.06	0.135	0.039	1.29	1.93	1.68	4.83	4.18	2.91	4.87

*Not used in rank sum or sign test.

Table B-2

RESULTS OF RANK SCORE AND SIGN TEST

Parameter		1		2		3		4		5		6	
Rank Score		47		49.5		58		66		59		58	
Sign Test Results	+	7/4	11	1/2	3	3/4	7	4/5	9	6/5	11	3/4	7
	0			1	1							1	1
	-	1/3	4	6/5	11	5/3	8	4/2	6	2/2	4	4/3	7

Parameter		7		8		9		10		11		12	
Rank Score		49		51		52.5		48.5		50.5		53	
Sign Test Results	+	3/2	5	3/1	4	1/2	3	3/1	4	1/1	2	1/1	2
	0			1	1	1/1	2	1	1	1	1	1	
	-	5/5	10	5/5	10	6/4	10	5/5	10	7/5	12	7/5	12

Parameter		13		14		15		16		17		18	
Rank Score		39.5		61.5		62		56		55.5		49	
Sign Test Results	+	3/1	4	6/6	12	3/3	6	4/3	7	5/4	9	5/3	8
	0							1	1				
	-	5/6	11	2/1	3	5/4	9	3/4	7	3/3	6	3/4	7

Parameter		19		20		21		22		23	
Rank Score		52		57		63.5		58.5		45	
Sign Test Results	+	2/3	5	3/4	7	2/2	4	3/2	5	4/1	5
	0	1	1			1	1	1/2	3	1/2	3
	-	5/4	9	5/3	8	6/4	10	4/3	7	3/4	7

Thus, the trend appears to continue in only half the cases.

Summarizing to this point; while the results of these tests are generally consistent with the hypothesis of no trend within sets, they also suggest that further study is in order. Thus, we intend to do one further analysis. When the general analysis of covariance is completed, we will include a trend term, presumed to be the same, within materials, and examine the results to see if this term materially affects the analysis. This will also remove any possible systematic trend in initial conditions.

B.2 LONG TERM TREND

The mean values for each material steadily decrease or increase for the first three materials. To examine this, we consider the mean values as reported for the orthogonal analysis. These are summarized in Table B-3 (with AL repeats displayed separately). Only a cursory examination is needed to see that any trend which might have been suggested by looking at AL, P, and T is not continued through steel.

The more interesting aspect of the data concerns a comparison between the initial aluminum set and the replicate set.

B.3 COMPARISON OF EARLY AND LATE AL RUNS

Early AL runs are compared with late AL runs using an analysis of variance, which includes a block effect.

This model hypothesizes that a systematic shift has occurred between the initial set of AL runs and the replicate set. Note that a large value of the lack of fit mean square, compared against pure error from replicates within sets, indicates that the model is inadequate. There are several potential factors which we will include in future analyses, such as initial conditions and time trend within sets. In addition, physical grounds exist which lead us to suspect that the very early runs (prior to run

Table B-3

MEANS BY MATERIAL

	AL (Early)	P	T	SS	AL (Late)
1	11.65	10	8.63	25.38	13.12
2	104.2	130.9	154.2	70.20	105.8
3	151.5	178	219	152.8	176.1
4	25.4	24.7	21.3	21.2	24.7
5	4.15	3.6	3.12	5.68	4.08
6	0.95	0.93	1.03	0.90	1.00
7	157	189	230	137	172
8	147	126	131	157	156
9	0.19	0.26	0.26	0.15	0.16
10	97.6	116.6	124.4	64.2	93.6
11	131.2	156.5	179.5	96.8	132.9
12	166.2	188.8	218.2	133.4	165.9
13	23.1	23.6	15.9	23.9	21.8
14	11.66	10.13	8.18	16.16	11.52
15	0.597	0.696	0.752	0.758	0.870
16	0.37	0.14	0.29	0.23	0.35
17	10.81	8.55	7.20	14.36	8.71
18	34.1	39.2	48.7	34.5	39.0
19	32.9	27.8	28.6	34.1	34.3
20	87.2	102.8	124.9	85.8	99.4
21	57.7	78.2	81.6	38.2	56.2
22	46.2	57.5	69.9	35.8	49.6
23	99.4	114.5	147.5	102.6	116.2

7), particularly run 5, may reflect differences in calibration or instrumentation. Thus, these results are preliminary until the full-scale covariance analysis is completed.

The format of the results in Table B-4 is as follows:

The components of variance are (1) the factorial model without a block effect; (2) the additional reduction due to adding the block effect into the model; (3) the residual variation after removing the pure error – this residual is a measure of lack of fit of the model, and (4) the pure error from replicates within sets.

	Degrees of Freedom	Sum of Squares	Mean Square
Factorial	8	–	
Block After Factors	1	–	
Residual (lack of fit)	7	–	
Pure Error	7	–	
Total	23	–	

The lack of fit (LOF) is deemed significant if the ratio:

$$\frac{\text{Mean Square LOF}}{\text{Mean Square Pure Error}} > F_{7,7,.95} = 3.79$$

If LOF is not significant, then the BLOCK effect is deemed significant if the ratio:

$$\frac{\text{Mean Square Blocks after Factors}}{\frac{(\text{Mean Square LOF} + \text{Mean Square Error})}{2}} > F_{1,14,.95} = 4.60$$

If LOF is significant, then the model is inadequate and no test for drift is made. Note, however, that if the ratio of

$$\frac{\text{Mean Square Blocks after Factors}}{\text{Mean Square LOF}} > F_{1,7,.95} = 5.59$$

there is reason to believe that a block effect is present.

Following are comments about Table B-4:

1. The results presented in Table B-4 have not yet been checked and hence should be considered preliminary.
2. Of the 23 parameters, 8 (1, 2, 4, 8, 12, 13, 21, and 22) exhibit no significant drift, while 5 (7, 15, 17, 20, 23) do exhibit significant drift. In particular, parameter 15 stands out in this regard. This is to be expected, since a basic change in the method of measuring 15 was made early in the program. Consequently, the early set, with respect to this parameter, should be discarded.
3. In the remaining 10 cases (3, 5, 6, 9, 10, 11, 14, 16, 18 and 19) there is significant lack of fit, which may be due to a variety of causes, as already discussed. We hope to resolve these cases when the more detailed analysis is completed. Note that among these 10 cases the mean square for block effect is generally small when compared to the residual, and one might anticipate that trend is not present in most cases.
4. Note that no long term drift is exhibited with respect to parameter 13, where previously a short term drift had been indicated. These two results are in conflict and our tentative conclusion is in favor of the NO drift hypothesis.

B.4 OVERALL CONCLUSIONS

We have found some evidence of trend or drift; however, no clear cut pattern nor explanation has yet emerged (except in the case of parameter 15). We will continue to examine the data in an effort to achieve a definite result.

Table B-4

VARIANCE ANALYSIS

Parameter	Source of Variation	Degree of Freedom	Sum of Squares	Mean Square	
1	Factorial Model	8	3751.6805		
	Blocks After Factorial	1	11.8225	11.8225	NS
	Residual	7	8.0692	1.1527	NS
	Error	7	23.9225	3.4175	
	Total	23	3799.4947		
2	Factorial Model	8	259944.3333		
	Blocks After Factorial	1	25.5569	25.5569	NS
	Residual	7	486.6098	69.5156	NS
	Error	7	537.5	76.7857	
	Total	23	261194.0		
3	Factorial Model	8	623107.9167		
	Blocks After Factorial	1	3424.4457	3424.4457	
	Residual	7	2682.4709	383.2101	*
	Error	7	628.1667	89.7381	
	Total	23	269843.0		
4	Factorial Model	8	15268.6142		
	Blocks After Factorial	1	11.0260	11.0260	NS
	Residual	7	112.5382	16.0769	NS
	Error	7	71.8616	10.2659	
	Total	23	15464.04		

NS = Not Significant

* = Significant

Table B-4 (Cont.)

Parameter	Source of Variation	Degree of Freedom	Sum of Squares	Mean Square	
5	Factorial Model	8	429.3611		
	Blocks After Factorial	1	0.2067	0.2067	
	Residual	7	2.1473	0.3067	*
	Error	7	0.2950	0.0421	
	Total	23	432.0101		
6	Factorial Model	8	22.2290		
	Blocks After Factorial	1	0.0052	0.0052	
	Residual	7	0.0053	0.00761	
	Error	7	0.0080	0.00114	*
	Total	23	22.2955		
7	Factorial Model	8	635802.5833		
	Blocks After Factorial	1	1357.3664	1357.3664	*
	Residual	7	1047.5503	149.6500	NS
	Error	7	528.5	75.5	
	Total	23	638736.0		
8	Factorial Model	8	547148.9167		
	Blocks After Factorial	1	181.0846	181.0846	NS
	Residual	7	1153.4987	164.7855	NS
	Error	7	434.5	62.0714	
	Total	23	54819.0		
9	Factorial Model	8	0.85934		
	Blocks After Factorial	1	0.00513	0.00513	
	Residual	7	0.03047	0.00435	*
	Error	7	0.00576	0.00082	
	Total	23	0.9007		

NS = Not Significant

* = Significant

Table B-4 (Cont.)

Parameter	Source of Variation	Degree of Freedom	Sum of Squares	Mean Square	
10	Factorial Model	8	214540.9167		
	Blocks After Factorial	1	37.3333	37.3333	
	Residual	7	1545.5833	220.7976	*
	Error	7	259.1667	37.0238	
	Total	23	216383.0		
11	Factorial Model	8	410467.25		
	Blocks After Factorial	1	17.4934	17.4934	
	Residual	7	1290.2566	184.3224	*
	Error	7	329.0	47.0	
	Total	23	412104.0		
12	Factorial Model	8	652365.0		
	Blocks After Factorial	1	0.0119	0.0119	NS
	Residual	7	1255.4880	179.3554	NS
	Error	7	351.5	50.2142	
	Total	23	653972.0		
13	Factorial Model	8	11691.208		
	Blocks After Factorial	1	7.560	7.560	NS
	Residual	7	23.972	3.4245	NS
	Error	7	18.75	2.6786	
	Total	23	11741.49		
14	Factorial Model	8	3196.2622		
	Blocks After Factorial	1	0.2177	0.2177	
	Residual	7	27.9736	3.9962	*
	Error	7	4.1498	0.5928	
	Total	23	3228.6033		

NS = Not Significant

* = Significant

Table B-4 (Cont.)

Parameter	Source of Variation	Degree of Freedom	Sum of Squares	Mean Square	
15	Factorial Model	8	12.1617		
	Blocks After Factorial	1	0.4291	0.4291	* (See Comment 2)
	Residual	7	0.0677	0.00967	NS
	Error	7	0.0178	0.00254	
	Total	23	12.0673		
16	Factorial Model	8	3.7977		
	Blocks After Factorial	1	0.0131	0.0131	
	Residual	7	0.7460	0.10657	*
	Error	7	0.0117	0.00167	
	Total	23	4.5867		
17	Factorial Model	8	2345.9945		
	Blocks After Factorial	1	29.1736	29.1736	*
	Residual	7	25.4453	3.6350	NS
	Error	7	9.5113	1.3588	
	Total	23	2410.1247		
18	Factorial Model	8	31159.8633		
	Blocks After Factorial	1	126.4612	126.4612	
	Residual	7	89.9039	12.8434	*
	Error	7	14.6816	2.0974	
	Total	23	31390.91		
19	Factorial Model	8	27095.1742		
	Blocks After Factorial	1	1.9201	1.9201	
	Residual	7	110.1157	15.7308	
	Error	7	20.35	2.9071	
	Total	23	27207.56		

NS = Not Significant

* = Significant

Table B-4 (Cont.)

Parameter	Source of Variation	Degree of Freedom	Sum of Squares	Mean Square	
20	Factorial Model	8	205760.6667		
	Blocks After Factorial	1	942.2433	942.2433	*
	Residual	7	517.4233	73.9176	NS
	Error	7	289.6667	41.3810	
	Total	23	207510.		
21	Factorial Model	8	76628.92		
	Blocks After Factorial	1	17.49	17.49	NS
	Residual	7	220.59	31.5128	NS
	Error	7	251.	35.8571	
	Total	23	77118.00		
22	Factorial Model	8			
	Blocks After Factorial	1	72.43	72.43	NS
	Residual	7	244.82	34.9743	NS
	Error	7	101.	14.4286	
	Total	23	55383.00		
23	Factorial Model	8	274151.56		
	Blocks After Factorial	1	1668.16	1668.16	*
	Residual	7	700.59	100.0843	NS
	Error	7	191.67	27.3814	
	Total	23	276712.00		

NS = Not Significant
* = Significant